3-30. Let $\mathbf{G}_4$ be the magnetic field of a z-directed current element situated $y > 0$ and radiating in the presence of a perfect electric conductor covering the $y = 0$ plane. In other words, let $\mathbf{c} = \mathbf{u}_z$ and S be the $y = 0$ plane. Show that

$$\mathbf{G}_4 = \nabla \times \mathbf{u}_z \left(\frac{e^{-jkr_1}}{r_1} - \frac{e^{-jkr_2}}{r_2} \right)$$

where

$$r_1 = \sqrt{(x - x')^2 + (y - y')^2 + (z - z')^2}$$
$$r_2 = \sqrt{(x - x')^2 + (y + y')^2 + (z - z')^2}$$

3-31. Specialize the $\mathbf{G}_4$ of Prob. 3-30 to $r_1 \to \infty$, and apply Eq. (3-57) to the problem of Fig. 3-28. Show that this gives the same answer as obtained in Prob. 3-19.

3-32. Apply duality to Eqs. (3-65), and evaluate the magnetic tensor Green's function [Γ] defined by

$$\mathbf{H} = [\Gamma]K\mathbf{l}$$

in free space.

3-33. Evaluate the Γ_{ij} for the free-space tensor Green's function defined by

$$\mathbf{H} = [\Gamma]\Pi$$

3-34. Repeat Prob. 3-20 using the physical optics approximation, and show that the answer for E_z^s differs from that of Prob. 3-20 by an interchange of ϕ and ϕ_0. Show that the echo area is identical to that of Prob. 3-20.

3-35. Repeat Prob. 3-21 using the physical optics approximation, and show that the answer for H_z^s differs from that of Prob. 3-21 by an interchange of ϕ and ϕ_0. Show that the echo area is identical to that of Prob. 3-21.

3-36. Let $\psi = e^{-jky}$ in Eqs. (3-86), and evaluate the electromagnetic field. Classify this field in as many ways as you can (wave-type, polarization, etc.).

3-37. Let $\psi = e^{-jkz}$ in Eqs. (3-89), and evaluate the electromagnetic field. Classify this field in as many ways as you can.

3-38. Let $\mathbf{c} = \mathbf{u}_z$, $\psi^a = e^{-jkz}$, $\psi^f = je^{-jkz}$, and evaluate Eqs. (3-91). Classify this field in as many ways as you can.

3-39. Derive Eqs. (3-97) by expanding Eqs. (3-4) with $\mathbf{A}$ and $\mathbf{F}$ as given by Eqs. (3-95).

CHAPTER 4

PLANE WAVE FUNCTIONS

4-1. The Wave Functions. The problems that we have considered so far are of two types: (1) those reducible to sources in an unbounded homogeneous region, and (2) those solvable by using one or more uniform plane waves. Equations (3-91) show us how to construct general solutions to the field equations in homogeneous regions once we have general solutions to the scalar Helmholtz equation. By a method called *separation of variables*, general solutions to the Helmholtz equation can be constructed in certain coordinate systems.[1] In this section, we use the method of separation of variables to obtain solutions for the rectangular coordinate system.

The Helmholtz equation in rectangular coordinates is

$$\frac{\partial^2\psi}{\partial x^2} + \frac{\partial^2\psi}{\partial y^2} + \frac{\partial^2\psi}{\partial z^2} + k^2\psi = 0 \tag{4-1}$$

The method of separation of variables seeks to find solutions of the form

$$\psi = X(x)Y(y)Z(z) \tag{4-2}$$

that is, solutions which are the product of three functions of one coordinate each. Substitution of Eq. (4-2) into Eq. (4-1), and division by ψ, yields

$$\frac{1}{X}\frac{d^2X}{dx^2} + \frac{1}{Y}\frac{d^2Y}{dy^2} + \frac{1}{Z}\frac{d^2Z}{dz^2} + k^2 = 0 \tag{4-3}$$

Each term can depend, at most, on only one coordinate. Since each coordinate can be varied independently, Eq. (4-3) can sum to zero for all coordinate values only if each term is independent of x, y, and z. Thus, let

$$\frac{1}{X}\frac{d^2X}{dx^2} = -k_x^2 \qquad \frac{1}{Y}\frac{d^2Y}{dy^2} = -k_y^2 \qquad \frac{1}{Z}\frac{d^2Z}{dz^2} = -k_z^2$$

where k_x, k_y, and k_z are constants, that is, are independent of x, y, and z. (The choice of minus a constant squared is taken for later convenience.)

[1] It has been shown by Eisenhart (*Ann. Math.*, vol. 35, p. 284, 1934) that the Helmholtz equation is separable in 11 three-dimensional orthogonal coordinate systems.

We now have Eq. (4-1) separated into the trio of equations

$$\begin{aligned} \frac{d^2X}{dx^2} + k_x^2 X &= 0 \\ \frac{d^2Y}{dy^2} + k_y^2 Y &= 0 \\ \frac{d^2Z}{dz^2} + k_z^2 Z &= 0 \end{aligned} \tag{4-4}$$

where, by Eq. (4-3), the separation parameters must satisfy

$$k_x^2 + k_y^2 + k_z^2 = k^2 \tag{4-5}$$

This last equation is called the *separation equation.*

Equations (4-4) are all of the same form. They will be called *harmonic equations.* Any solution to the harmonic equation we shall call a *harmonic function,*[1] and denote it, in general, by $h(k_x x)$. Commonly used harmonic functions are

$$h(k_x x) \sim \sin k_x x,\ \cos k_x x,\ e^{jk_x x},\ e^{-jk_x x} \tag{4-6}$$

Any two of these are linearly independent. A constant times a harmonic function is still a harmonic function. A sum of harmonic functions is still a harmonic function. From Eqs. (4-2) and (4-4) it is evident that

$$\psi_{k_x k_y k_z} = h(k_x x)h(k_y y)h(k_z z) \tag{4-7}$$

are solutions to the Helmholtz equation when the k_i satisfy Eq. (4-5). These solutions are called *elementary wave functions.*

Linear combinations of the elementary wave functions must also be solutions to the Helmholtz equation. As evidenced by Eq. (4-5), only two of the k_i may be chosen independently. We can therefore construct more general wave functions by summing over possible choices for one or two separation parameters. For example,

$$\begin{aligned} \psi &= \sum_{k_x} \sum_{k_y} B_{k_x k_y} \psi_{k_x k_y k_z} \\ &= \sum_{k_x} \sum_{k_y} B_{k_x k_y} h(k_x x)h(k_y y)h(k_z z) \end{aligned} \tag{4-8}$$

where the B_{ij} are constants, is a solution to the Helmholtz equation. The values of the k_i needed for any particular problem are determined by the boundary conditions of the problem and are called *eigenvalues* or *characteristic values.* The elementary wave functions corresponding to specific eigenvalues are called *eigenfunctions.*

[1] The term *harmonic function* also is used to denote a solution to Laplace's equation. This is not the present meaning of the term.

Still more general wave functions can be constructed by integrating over one or two of the k_i. For example, a solution to the Helmholtz equation is

$$\begin{aligned} \psi &= \int_{k_x} \int_{k_y} f(k_x,k_y)\psi_{k_x k_y k_z}\, dk_x\, dk_y \\ &= \int_{k_x} \int_{k_y} f(k_x,k_y)h(k_x x)h(k_y y)h(k_z z)\, dk_x\, dk_y \end{aligned} \tag{4-9}$$

where $f(k_x,k_y)$ is an analytic function, and the integration is over any path in the complex k_x and k_y domains. Equation (4-9) exhibits a continuous variation of the separation parameters, and we say that there exists a continuous spectrum of eigenvalues. We shall see that solutions for finite regions (waveguides and cavities) are characterized by discrete spectra of eigenvalues, while solutions for unbounded regions (antennas) often require continuous spectra. Wave functions of the form of Eq. (4-9) are most commonly used to construct Fourier integrals.

We should be familiar with the mathematical properties and with the physical interpretations of the various harmonic functions so that we can properly choose them for particular problems. Keep in mind that wave functions represent instantaneous quantities, according to Eq. (1-40). Solutions of the form $h(kx) = e^{-jkx}$ (k positive real) represent waves traveling unattenuated in the $+x$ direction. If k is complex and Re $(k) > 0$, we have $+x$ traveling waves which are attenuated or augmented according as Im (k) is negative or positive. Similarly, solutions of the form $h(kx) = e^{jkx}$, [Re $(k) > 0$] represent $-x$ traveling waves, attenuated or augmented if k is complex. If k is purely imaginary, the above two harmonic functions represent evanescent fields. Solutions of the form $h(kx) = \sin kx$ and $h(kx) = \cos kx$ with k real represent pure standing waves. If k is complex, they represent localized standing waves. If k is purely imaginary, say $k = -j\alpha$ with α real, then the "trigonometric functions" sin kx and cos kx can be expressed as "hyperbolic functions" sinh αx and cosh αx. We should get used to thinking of the various functions as defined over the entire complex kx plane. The trigonometric and hyperbolic functions are then just specializations of the complex harmonic functions. Table 4-1 summarizes the above discussion. (The convention $k = \beta - j\alpha$ with α and β real is used.) Note that the degenerate case $k = 0$ has the harmonic functions $h(0x) = 1,x$. The choice of the proper harmonic functions in any particular case is largely a matter of experience, and facility in this respect will be gained as we use them.

4-2. Plane Waves. Consider an elementary wave function of the form

$$\psi = e^{-jk_x x}e^{-jk_y y}e^{-jk_z z} \tag{4-10}$$

TABLE 4-1. PROPERTIES OF THE HARMONIC FUNCTIONS*

$h(kx)$	Zeros†	Infinities†	Specializations of $k = \beta - j\alpha$	Special representations	Physical interpretation
e^{-jkx}	$kx \to -j\infty$	$kx \to j\infty$	k real k imaginary k complex	$e^{-j\beta x}$ $e^{-\alpha x}$ $e^{-\alpha x}e^{-j\beta x}$	$+x$ traveling wave Evanescent field Attenuated traveling wave
e^{jkx}	$kx \to j\infty$	$kx \to -j\infty$	k real k imaginary k complex	$e^{j\beta x}$ $e^{\alpha x}$ $e^{\alpha x}e^{j\beta x}$	$-x$ traveling wave Evanescent field Attenuated traveling wave
$\sin kx$	$kx = n\pi$	$kx \to \pm j\infty$	k real k imaginary k complex	$\sin \beta x$ $-j \sinh \alpha x$ $\sin \beta x \cosh \alpha x$ $-j \cos \beta x \sinh \alpha x$	Standing wave. Two evanescent fields Localized standing waves
$\cos kx$	$kx = (n + \frac{1}{2})\pi$	$kx \to \pm j\infty$	k real k imaginary k complex	$\cos \beta x$ $\cosh \alpha x$ $\cos \beta x \cosh \alpha x$ $+j \sin \beta x \sinh \alpha x$	Standing wave Two evanescent fields Localized standing waves

* For $k = 0$, the harmonic functions are $h(0x) = 1, x$.
† For an essential singularity, this column gives the asymptotic behavior.

The k_i must satisfy Eq. (4-5), which is of the form of the scalar product of a vector

$$\mathbf{k} = \mathbf{u}_x k_x + \mathbf{u}_y k_y + \mathbf{u}_z k_z \tag{4-11}$$

with itself. Note that in terms of $\mathbf{k}$ and the radius vector

$$\mathbf{r} = \mathbf{u}_x x + \mathbf{u}_y y + \mathbf{u}_z z \tag{4-12}$$

we can express Eq. (4-10) as

$$\psi = e^{-j\mathbf{k}\cdot\mathbf{r}} \tag{4-13}$$

For $\mathbf{k}$ real, we apply Eq. (2-140) and determine the vector phase constant

$$\boldsymbol{\beta} = -\nabla(-\mathbf{k}\cdot\mathbf{r}) = \mathbf{k}$$

Hence, the equiphase surfaces are planes perpendicular to $\mathbf{k}$. The amplitude of the wave is constant (unity). Equation (4-13) therefore represents a scalar uniform plane wave propagating in the direction of $\mathbf{k}$. Figure 4-1 illustrates this interpretation.

For $\mathbf{k}$ complex, we define two real vectors

$$\mathbf{k} = \boldsymbol{\beta} - j\boldsymbol{\alpha} \tag{4-14}$$

and determine the vector propagation constant according to Eq. (2-145). This gives

$$\boldsymbol{\gamma} = -\nabla(-j\mathbf{k}\cdot\mathbf{r}) = j\mathbf{k} = \boldsymbol{\alpha} + j\boldsymbol{\beta}$$

We now have equiphase surfaces perpendicular to $\boldsymbol{\beta}$ and equiamplitude surfaces perpendicular to $\boldsymbol{\alpha}$. Thus, when $\mathbf{k}$ is complex, Eq. (4-13) represents a plane wave propagating in the direction of $\boldsymbol{\beta}$ and attenuating in the direction of $\boldsymbol{\alpha}$. It is a uniform plane wave only if $\boldsymbol{\beta}$ and $\boldsymbol{\alpha}$ are in the same direction. Note that definitions $\mathbf{k} = \boldsymbol{\beta} - j\boldsymbol{\alpha}$ and $k = k' - jk''$ do *not* imply that β equals k' or that α equals k'' in general. In fact, for loss-free media,

$$k^2 = \mathbf{k}\cdot\mathbf{k} = \beta^2 - \alpha^2 - j2\boldsymbol{\alpha}\cdot\boldsymbol{\beta}$$

must be positive real. Hence, either $\boldsymbol{\alpha} = 0$ or $\boldsymbol{\alpha}\cdot\boldsymbol{\beta} = 0$. When $\boldsymbol{\alpha} = 0$ we have the uniform plane wave discussed above. When $\boldsymbol{\alpha}$ and $\boldsymbol{\beta}$ are mutually orthogonal we have an evanescent field, such as was encountered in total reflection [Eq. (2-62)].

The elementary wave functions of Eq. (4-10) or Eq. (4-13) are quite general, since sinusoidal wave functions are linear combinations of the exponential wave functions. Wave functions of the type of Eqs. (4-8) and (4-9) are linear combinations of the elementary wave functions. We therefore conjecture that all wave functions can be expressed as superpositions of plane waves.

Let us now consider the electromagnetic fields that we can construct from the wave functions of Eq. (4-10). Fields TM to z are obtained if ψ is interpreted according to $\mathbf{A} = \mathbf{u}_z\psi$. This choice results in Eqs. (3-86), which, for the ψ of Eq. (4-10), become

$$\begin{aligned}\mathbf{H} &= -\mathbf{u}_x jk_y\psi + \mathbf{u}_y jk_x\psi \\ &= \nabla\psi \times \mathbf{u}_z = j\psi\mathbf{u}_z \times \mathbf{k}\end{aligned} \tag{4-15}$$

and

$$\begin{aligned}\hat{y}\mathbf{E} &= jk_z(\mathbf{u}_x jk_x + \mathbf{u}_y jk_y + \mathbf{u}_z jk_z)\psi + \mathbf{u}_z k^2\psi \\ &= (-k_z\mathbf{k} + \mathbf{u}_z k^2)\psi\end{aligned} \tag{4-16}$$

For $\mathbf{k}$ real, $\mathbf{H}$ is perpendicular to $\mathbf{k}$ by Eq. (4-15), and $\mathbf{E}$ is perpendicular to $\mathbf{k}$, since

$$\hat{y}\mathbf{k}\cdot\mathbf{E} = (-k_z k^2 + k_z k^2)\psi = 0$$

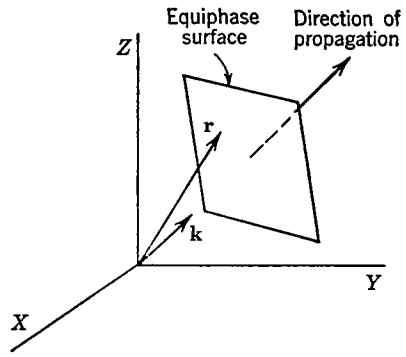

FIG. 4-1. A uniform plane wave.

Thus, the wave is TEM to the direction of propagation (as well as TM to z). For $\mathbf{k}$ complex, define α and β by Eq. (4-14). It then follows that the wave is not necessarily TEM to the direction of propagation (that of β). It will be TEM to β only if α and β are in the same direction, that is, if

$$\mathbf{k} = \beta - j\alpha = (\mathbf{u}_x l + \mathbf{u}_y m + \mathbf{u}_z n)k$$

with l, m, n real. In this case, $\beta = k'$, $\alpha = k''$, and l, m, n are the direction cosines.

The dual procedure applies when ψ is interpreted according to $\mathbf{F} = \mathbf{u}_z\psi$. In this case, Eqs. (3-89) apply, giving

$$\begin{aligned} \mathbf{E} &= j\psi\mathbf{k} \times \mathbf{u}_z \\ \hat{z}\mathbf{H} &= (-k_z\mathbf{k} + \mathbf{u}_z k^2)\psi \end{aligned} \tag{4-17}$$

which are dual to Eqs. (4-15) and (4-16). For k real, this is a wave TEM to $\mathbf{k}$ and TE to z. Its polarization is orthogonal to the corresponding TM-to-z wave. For $\mathbf{k}$ complex, the wave is not necessarily TEM to the direction of propagation. All these fields are plane waves. An arbitrary electromagnetic field in a homogeneous region can be considered as a superposition of these plane waves.

4-3. The Rectangular Waveguide. The problem of determining modes in a rectangular waveguide provides a good illustration of the use of elementary wave functions. In Sec. 2-7 we considered only the dominant mode. In this section we shall consider the complete mode spectrum. The geometry of the rectangular waveguide is illustrated by Fig. 2-16.

It is conventional to classify the modes in a rectangular waveguide as TM to z (no H_z) and TE to z (no E_z). Modes TM to z are expressible in terms of an $\mathbf{A}$ having only a z component ψ. We wish to consider traveling waves; hence we consider wave functions of the form

$$\psi = h(k_x x)h(k_y y)e^{-jk_z z} \tag{4-18}$$

The electromagnetic field is given by Eqs. (3-86). In particular,

$$E_z = \frac{1}{\hat{y}}(k^2 - k_z^2)\psi$$

The boundary conditions on the problem are that tangential components of $\mathbf{E}$ vanish at the conducting walls. Hence, E_z must be zero at $x = 0$, $x = a$, $y = 0$, and $y = b$. The only harmonic functions having two or more zeros are the sinusoidal functions with k_i real. Thus, choose

$$h(k_x x) = \sin k_x x \qquad k_x = \frac{m\pi}{a} \qquad m = 1, 2, 3, \ldots$$

$$h(k_y y) = \sin k_y y \qquad k_y = \frac{n\pi}{b} \qquad n = 1, 2, 3, \ldots$$

so that the boundary conditions on E_z are satisfied. Each integer m and n specifies a possible field, or mode. The TM_{mn} *mode functions* are therefore

$$\psi_{mn}{}^{\mathrm{TM}} = \sin\frac{m\pi x}{a}\sin\frac{n\pi y}{b}e^{-jk_z z} \tag{4-19}$$

with $m = 1, 2, 3, \ldots$, and $n = 1, 2, 3, \ldots$, and the separation parameter equation [Eq. (4-5)] becomes

$$\left(\frac{m\pi}{a}\right)^2 + \left(\frac{n\pi}{b}\right)^2 + k_z^2 = k^2 \tag{4-20}$$

The TM_{mn} mode fields are obtained by substituting the $\psi_{mn}{}^{\mathrm{TM}}$ into Eqs. (3-86).

Modes TE to z are expressible in terms of an $\mathbf{F}$ having only a z component ψ. Again, we wish to find traveling waves; so the ψ must be of the form of Eqs. (4-18). The electromagnetic field this time will be given by Eqs. (3-89). In particular,

$$E_x = -\frac{\partial\psi}{\partial y} \qquad E_y = \frac{\partial\psi}{\partial x}$$

the first of which must vanish at $y = 0$, $y = b$, and the second at $x = 0$, $x = a$. Harmonic functions satisfying these boundary conditions are

$$h(k_x x) = \cos k_x x \qquad k_x = \frac{m\pi}{a} \qquad m = 0, 1, 2, \ldots$$

$$h(k_y y) = \cos k_y y \qquad k_y = \frac{n\pi}{b} \qquad n = 0, 1, 2, \ldots$$

Each integer m and n, except $m = n = 0$ (in which case $\mathbf{E}$ vanishes identically), specifies a mode. Hence, the TE_{mn} mode functions are

$$\psi_{mn}{}^{\mathrm{TE}} = \cos\frac{m\pi x}{a}\cos\frac{n\pi y}{b}e^{-jk_z z} \tag{4-21}$$

with $m = 0, 1, 2, \ldots$; $n = 0, 1, 2, \ldots$; $m = n = 0$ excepted. The separation parameter equation remains the same as in the TM case [Eq. (4-20)]. The TE_{mn} mode fields are obtained by substituting the $\psi_{mn}{}^{\mathrm{TE}}$ into Eqs. (3-89).

Interpretation of each mode is similar to that of the dominant TE_{01} mode, considered in Sec. 2-7. Equation (4-20) determines the mode propagation constant $\gamma = jk_z$. For k real, the propagation constant vanishes when k is

$$\sqrt{\left(\frac{m\pi}{a}\right)^2 + \left(\frac{n\pi}{b}\right)^2} = (k_c)_{mn} \tag{4-22}$$

The $(k_c)_{mn}$ is called the *cutoff wave number* of the mn mode. For other values of k, we have

$$\gamma_{mn} = jk_z = \begin{cases} j\beta = j\sqrt{k^2 - (k_c)_{mn}^2} & k > k_c \\ \alpha = \sqrt{(k_c)_{mn}^2 - k^2} & k < k_c \end{cases} \tag{4-23}$$

Thus, for $k > k_c$ the mode is propagating, and for $k < k_c$ the mode is nonpropagating (evanescent). From Eq. (4-22) we determine the cutoff frequencies

$$(f_c)_{mn} = \frac{k_c}{2\pi\sqrt{\epsilon\mu}} = \frac{1}{2\sqrt{\epsilon\mu}}\sqrt{\left(\frac{m}{a}\right)^2 + \left(\frac{n}{b}\right)^2} \tag{4-24}$$

and the cutoff wavelengths

$$(\lambda_c)_{mn} = \frac{2\pi}{k_c} = \frac{2}{\sqrt{(m/a)^2 + (n/b)^2}} \tag{4-25}$$

In terms of the cutoff frequencies, we can re-express the mode propagation constants as

$$\gamma = jk_z = \begin{cases} j\beta = jk\sqrt{1 - \left(\frac{f_c}{f}\right)^2} & f > f_c \\ \alpha = k_c\sqrt{1 - \left(\frac{f}{f_c}\right)^2} & f < f_c \end{cases} \tag{4-26}$$

where mode indices mn are implied. We can also define mode wavelengths for each mode by Eq. (2-85) and mode phase velocities by Eq. (2-86), where mode indices are again implied.

It is apparent that $\gamma = jk_z$ for each mode has the same interpretation as γ for the TE_{01} mode. It is the physical size (compared to wavelength) of the waveguide that determines which modes propagate. Table 4-2 gives a tabulation of some of the smaller eigenvalues for various ratios b/a. Whenever two or more modes have the same cutoff frequency, they are said to be *degenerate modes*. The corresponding TE_{mn} and TM_{mn} modes are always degenerate in the rectangular guide (but not in other-shaped guides). In the square guide ($b/a = 1$), the TE_{mn}, TE_{nm}, TM_{mn}, and TM_{nm} modes form a foursome of degeneracy. Waveguides are usually constructed so that only one mode propagates, hence $b/a > 1$ usually. For $b/a = 2$, we have a 2:1 frequency range of single-mode operation, and this is the most common practical geometry. It is undesirable to make b/a greater than 2 for high-power operation, since, if the guide is too thin, arcing may occur. (The breakdown power is proportional to $\sqrt{a}$ for fixed b.) To illustrate the use of Table 4-2, suppose we wish to design an air-filled waveguide to propagate the TE_{01} mode at 10,000 megacycles ($\lambda = 3$ centimeters). We do not wish to operate too close to f_c, since the conductor losses are then large (see Table 2-4). If we take

TABLE 4-2. $\frac{(k_c)_{mn}}{(k_c)_{01}} = \frac{(f_c)_{mn}}{(f_c)_{01}} = \frac{(\lambda_c)_{01}}{(\lambda_c)_{mn}}$ FOR THE RECTANGULAR WAVEGUIDE, $b \geq a$

$\frac{b}{a}$	TE_{01}	TE_{10}	TE_{11} TM_{11}	TE_{02}	TE_{20}	TE_{12} TM_{12}	TE_{21} TM_{21}	TE_{22} TM_{22}	TE_{03}
1	1	1	1.414	2	2	2.236	2.236	2.828	3
1.5	1	1.5	1.803	2	3	2.500	3.162	3.606	3
2	1	2	2.236	2	4	2.828	4.123	4.472	3
3	1	3	3.162	2	6	3.606	6.083	6.325	3
∞	1	∞	∞	2	∞	∞	∞	∞	3

$b = 2$ centimeters, then $\lambda_c = 4$ centimeters for the TE_{01} mode, and we are operating well above cutoff. The next modes to become propagating are the TE_{10} and TE_{02} modes, at a frequency of 15,000 megacycles. The TE_{11} and TM_{11} modes become propagating at 16,770 megacycles, and so on.

The mode patterns (field lines) are also of interest. For this, we determine **E** and **H** from Eqs. (3-86) and (4-19) or Eqs. (3-89) and (4-21), and then determine $\mathcal{E}$, $\mathcal{H}$ from Eq. (1-41). The mode pattern is a plot of lines of $\mathcal{E}$ and $\mathcal{H}$ at some instant. (A more direct procedure for obtaining the mode patterns is considered in Sec. 8-1.) Figure 4-2 shows sketches of cross-sectional mode patterns for some of the lower-order modes. When a line appears to end in space in these patterns, it actually loops down the guide. A more complete picture is shown for the TE_{01} mode in Fig. 2-17.

In addition, each mode is characterized by a constant (with respect to

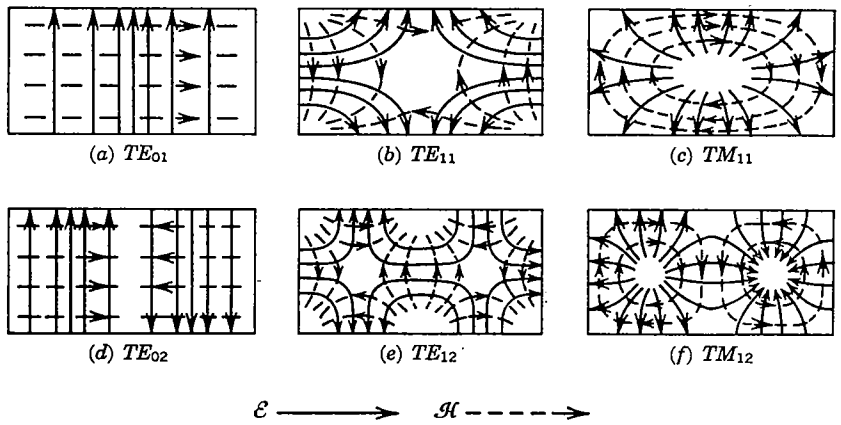

FIG. 4-2. Rectangular waveguide mode patterns.

x, y) z-directed wave impedance. For the TE_{mn} modes in loss-free media, we have from Eqs. (3-89) and (4-21)

$$j\omega\mu H_x = -jk_z \frac{\partial\psi}{\partial x} = -jk_z E_y$$

$$j\omega\mu H_y = -jk_z \frac{\partial\psi}{\partial y} = jk_z E_x$$

The TE_{mn} characteristic wave impedances are therefore

$$(Z_0)_{mn}{}^{TE} = \frac{E_x}{H_y} = -\frac{E_y}{H_x} = \frac{\omega\mu}{k_z} = \begin{cases} \dfrac{\omega\mu}{\beta} & f > f_c \\ \dfrac{j\omega\mu}{\alpha} & f < f_c \end{cases} \tag{4-27}$$

Similarly, for the TM_{mn} modes, we have from Eqs. (3-86) and (4-19)

$$j\omega\epsilon E_x = -jk_z \frac{\partial\psi}{\partial x} = jk_z H_y$$

$$j\omega\epsilon E_y = -jk_z \frac{\partial\psi}{\partial y} = -jk_z H_x$$

Thus, the TM_{mn} characteristic wave impedances are

$$(Z_0)_{mn}{}^{TM} = \frac{E_x}{H_y} = \frac{-E_y}{H_x} = \frac{k_z}{\omega\epsilon} = \begin{cases} \dfrac{\beta}{\omega\epsilon} & f > f_c \\ \dfrac{\alpha}{j\omega\epsilon} & f < f_c \end{cases} \tag{4-28}$$

It is interesting to note that the product $(Z_0)_{mn}{}^{TE}(Z_0)_{mn}{}^{TM} = \eta^2$ at all frequencies. By Eq. (4-26), $\beta < k$ for propagating modes; so the TE characteristic wave impedances are always greater than η, and the TM characteristic wave impedances are always less than η. For nonpropagating modes, the TE characteristic impedances are inductive, and the TM characteristic impedances are capacitive. Figure 4-3 illustrates this behavior.

Attenuation of the higher-order modes due to dielectric losses is given by the same formula as for the dominant mode (see Table 2-4). Attenuation due to conductor losses is given in Prob. 4-4.

4-4. Alternative Mode Sets. The classification of waveguide modes into sets TE or TM to z is important because it applies also to guides of nonrectangular cross section. However, for many rectangular waveguide problems, more convenient classifications can be made. We now consider these alternative sets of modes.

If, instead of Eq. (3-84), we choose

$$\mathbf{A} = \mathbf{u}_x\psi \tag{4-29}$$

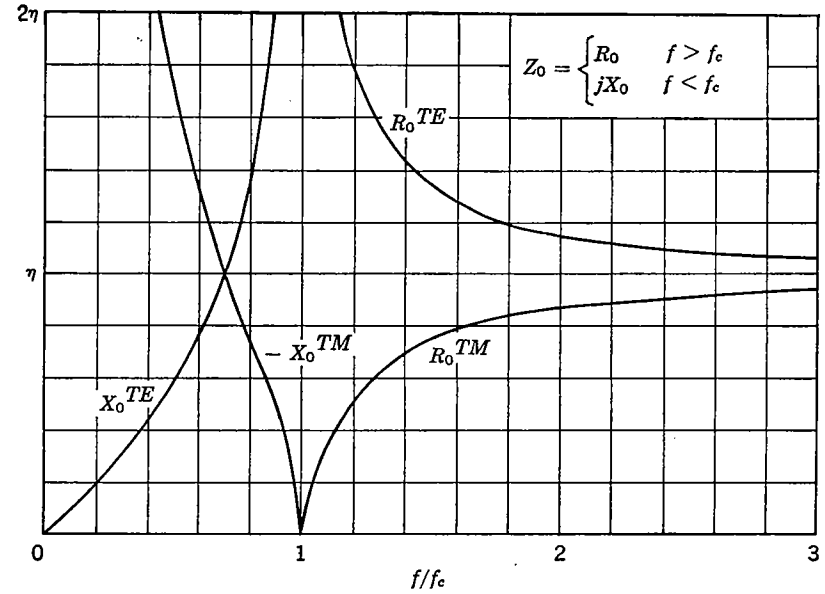

FIG. 4-3. Characteristic impedance of waveguide modes.

we have an electromagnetic field given by a set of equations differing from Eqs. (3-86) by a cyclic interchange of x, y, z. To be specific, the field is given by

$$\begin{aligned} E_x &= \frac{1}{\hat{y}}\left(\frac{\partial^2}{\partial x^2} + k^2\right)\psi & H_x &= 0 \\ E_y &= \frac{1}{\hat{y}}\frac{\partial^2\psi}{\partial x\,\partial y} & H_y &= \frac{\partial\psi}{\partial z} \\ E_z &= \frac{1}{\hat{y}}\frac{\partial^2\psi}{\partial x\,\partial z} & H_z &= -\frac{\partial\psi}{\partial y} \end{aligned} \tag{4-30}$$

This field is TM to x. Similarly, if, instead of Eq. (3-87), we choose

$$\mathbf{F} = \mathbf{u}_x\psi \tag{4-31}$$

we have an electromagnetic field given by

$$\begin{aligned} E_x &= 0 & H_x &= \frac{1}{\hat{z}}\left(\frac{\partial^2}{\partial x^2} + k^2\right)\psi \\ E_y &= -\frac{\partial\psi}{\partial z} & H_y &= \frac{1}{\hat{z}}\frac{\partial^2\psi}{\partial x\,\partial y} \\ E_z &= \frac{\partial\psi}{\partial y} & H_z &= \frac{1}{\hat{z}}\frac{\partial^2\psi}{\partial x\,\partial z} \end{aligned} \tag{4-32}$$

This field is TE to x. According to the concepts of Sec. 3-12, an arbitrary field can be constructed as a superposition of Eqs. (4-30) and (4-32).

The choice of ψ's to satisfy the boundary conditions for the rectangular waveguide (Fig. 2-16) is relatively simple. For modes TM to x (TMx_{mn} modes) we have

$$\psi_{mn}^{\text{TM}x} = \cos\frac{m\pi x}{a}\sin\frac{n\pi y}{b}\,e^{-jk_z z} \tag{4-33}$$

where $m = 0, 1, 2, \ldots$; $n = 1, 2, 3, \ldots$; and k_z is given by Eq. (4-26). The electromagnetic field is found by substituting Eq. (4-33) into Eqs. (4-30). For modes TE to x (TEx_{mn} modes) we have

$$\psi_{mn}^{\text{TE}x} = \sin\frac{m\pi x}{a}\cos\frac{n\pi y}{b}\,e^{-jk_z z} \tag{4-34}$$

where $m = 1, 2, 3, \ldots$; $n = 0, 1, 2, \ldots$; and k_z is again given by Eq. (4-26). The field is obtained by substituting Eq. (4-34) into Eqs. (4-32). Note that the TMx_{0n} modes are the TE$_{0n}$ modes of Sec. 4-3, and the TEx_{m0} modes are the TE$_{m0}$ modes. All other modes of Eqs. (4-33) and (4-34) are linear combinations of the degenerate sets of TE and TM modes. Note that our present set of modes have both an E_z and H_z (except for the 0-order modes). Such modes are called *hybrid*.

The mode patterns of these hybrid modes can be determined in the usual manner. (Determine **E**, **H**, then $\mathcal{E}$, $\mathcal{H}$, and specialize to some instant of time.) The TEx_{m0} mode patterns are those of the TE$_{m0}$ modes, and the TMx_{0n} mode patterns are those of the TE$_{0n}$ modes. Figure 4-4 shows the mode patterns for the TEx_{11} and TMx_{11} modes, to illustrate the character of the higher-order mode patterns.

The characteristic impedances of the hybrid modes are also of interest. For the TMx modes, we have from Eqs. (4-30) and (4-33)

$$j\omega\epsilon E_x = \left[k^2 - \left(\frac{m\pi}{a}\right)^2\right]\psi \qquad H_y = -jk_z\psi$$

Hence, the z-directed wave impedances are

$$(Z_0)_{mn}^{\text{TM}x} = \frac{E_x}{H_y} = \frac{k^2 - (m\pi/a)^2}{\omega\epsilon k_z} = \begin{cases} \dfrac{k^2 - (m\pi/a)^2}{\omega\epsilon\beta} & f > f_c \\ \dfrac{k^2 - (m\pi/a)^2}{-j\omega\epsilon\alpha} & f < f_c \end{cases} \tag{4-35}$$

Note that for a small, the cutoff TMx_{mn} modes, $m \neq 0$, have capacitive Z_0's, while the cutoff TMx_{0n} modes have inductive Z_0's. Similarly, from

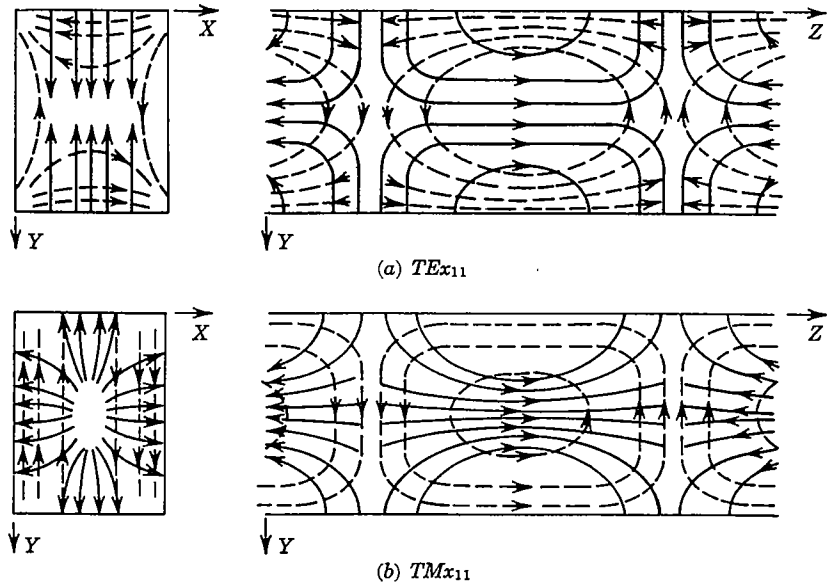

FIG. 4-4. Hybrid mode patterns.

Eqs. (4-32) and (4-34) we find

$$(Z_0)_{mn}^{\text{TE}x} = \frac{-E_y}{H_x} = \frac{\omega\mu k_z}{k^2 - (m\pi/a)^2} = \begin{cases} \dfrac{\omega\mu\beta}{k^2 - (m\pi/a)^2} & f > f_c \\ \dfrac{-j\omega\mu\alpha}{k^2 - (m\pi/a)^2} & f < f_c \end{cases} \tag{4-36}$$

Note that for a small, the cutoff TEx_{mn} modes all have inductive characteristic impedances.

Sets of modes TM and TE to y can be determined by letting $\mathbf{A} = \mathbf{u}_y\psi$ and $\mathbf{F} = \mathbf{u}_y\psi$, respectively. The fields would be given by equations similar to Eqs. (4-30) and (4-32) with x, y, z properly interchanged. The TMy and TEy mode functions would be given by Eqs. (4-33) and (4-34) with mx/a and ny/b interchanged.

4-5. The Rectangular Cavity. We considered the dominant mode of the rectangular cavity in Sec. 2-8. We shall now consider the complete mode spectrum. The geometry of the rectangular cavity is illustrated by Fig. 2-19.

The problem is symmetrical in x, y, z; so we can express the fields as TE or TM to any one of these coordinates. It is conventional to choose the z coordinate, and then the cavity modes are standing waves of the usual TE and TM waveguide modes. The wave functions of Eq. (4-19)

satisfy the boundary condition of zero tangential **E** at four of the walls. It is merely necessary to repick $h(k_z z)$ to satisfy this condition at the remaining two walls. This is evidently accomplished if

$$\psi_{mnp}^{\text{TM}} = \sin\frac{m\pi x}{a}\sin\frac{n\pi y}{b}\cos\frac{p\pi z}{c} \tag{4-37}$$

with $m = 1, 2, 3, \ldots$; $n = 1, 2, 3, \ldots$; $p = 0, 1, 2, \ldots$; and Eq. (4-20) becomes

$$\left(\frac{m\pi}{a}\right)^2 + \left(\frac{n\pi}{b}\right)^2 + \left(\frac{p\pi}{c}\right)^2 = k^2 \tag{4-38}$$

The field of the TM_{mnp} mode is given by substitution of Eq. (4-37) into Eqs. (3-86). Similarly, the TE_{mnp} mode functions are given by

$$\psi_{mnp}^{\text{TE}} = \cos\frac{m\pi x}{a}\cos\frac{n\pi y}{b}\sin\frac{p\pi z}{c} \tag{4-39}$$

with $m = 0, 1, 2, \ldots ; n = 0, 1, 2, \ldots ; p = 1, 2, 3, \ldots ; m = n = 0$ excepted. The separation equation remains Eq. (4-38). The TE_{mnp} mode field is given by substitution of Eq. (4-39) into Eqs. (3-89).

As indicated by Eq. (4-38), each mode can exist at only a single k, given a, b, c. Setting $k = 2\pi f\sqrt{\epsilon\mu}$, we solve Eq. (4-38) for the resonant frequencies

$$(f_r)_{mnp} = \frac{1}{2\sqrt{\epsilon\mu}}\sqrt{\left(\frac{m}{a}\right)^2 + \left(\frac{n}{b}\right)^2 + \left(\frac{p}{c}\right)^2} \tag{4-40}$$

For $a < b < c$, the dominant mode is the TE_{011} mode. Table 4-3 gives the ratio $(f_r)_{mnp}/(f_r)_{011}$ for cavities of various side lengths. Note that

TABLE 4-3. $\dfrac{(f_r)_{mnp}}{(f_r)_{011}}$ FOR THE RECTANGULAR CAVITY, $a \le b \le c$

$\frac{b}{a}$	$\frac{c}{a}$	TE_{011}	TE_{101}	TM_{110}	TM_{111} TE_{111}	TE_{012}	TE_{021}	TE_{201}	TE_{102}	TM_{120}	TM_{210}	TM_{112} TE_{112}
1	1	1	1	1	1.22	1.58	1.58	1.58	1.58	1.58	1.58	1.73
1	2	1	1	1.26	1.34	1.26	1.84	1.84	1.26	2.00	2.00	1.55
2	2	1	1.58	1.58	1.73	1.58	1.58	2.91	2.00	2.00	2.91	2.12
2	4	1	1.84	2.00	2.05	1.26	1.84	3.60	2.00	2.53	3.68	2.19
4	4	1	2.91	2.91	3.00	1.58	1.58	5.71	3.16	3.16	5.71	3.24
4	8	1	3.62	3.65	3.66	1.26	1.84	7.20	3.65	4.03	7.25	3.82
4	16	1	3.88	4.00	4.01	1.08	1.96	7.76	3.91	4.35	7.83	4.13

the TE_{mnp} and TM_{mnp} modes, mnp all nonzero, are always degenerate. When two or more sides of the cavity are of equal length, still other degeneracies occur. The greatest separation between the dominant mode and the next lowest-order mode is obtained for a square-base cavity ($b = c$) with height one-half or less of the base length ($b/a \ge 2$). In this case, the second resonance is $\sqrt{5/2} = 1.58$ times the first resonance.

The mode patterns of the rectangular cavity are similar to those of the TE or TM waveguide modes in a z = constant plane, and similar to the hybrid mode patterns in the other two cross sections. The most significant difference between the waveguide patterns and the cavity patterns is that $\mathcal{E}$ is shifted from $\mathcal{H}$ by $\lambda_g/4$ in the latter case. Also, $\mathcal{E}$ and $\mathcal{H}$ are 90° out of phase in a cavity; so $\mathcal{E}$ is zero when $\mathcal{H}$ is maximum, and vice versa. The TE_{011} mode pattern is shown in Fig. 2-20. To illustrate higher-order mode patterns, Fig. 4-5 shows the TE_{123} mode pattern.

The quality factor Q of each cavity mode can be determined by the method used in Sec. 2-8 for the dominant mode. The Q due to dielectric losses is the same for all modes, given by Eq. (2-100). The Q's due to conductor losses for the various modes are given in Prob. 4-10. Note that the Q increases as the mode order increases. The Q varies roughly as the ratio of volume to surface area of the cavity, since the energy is

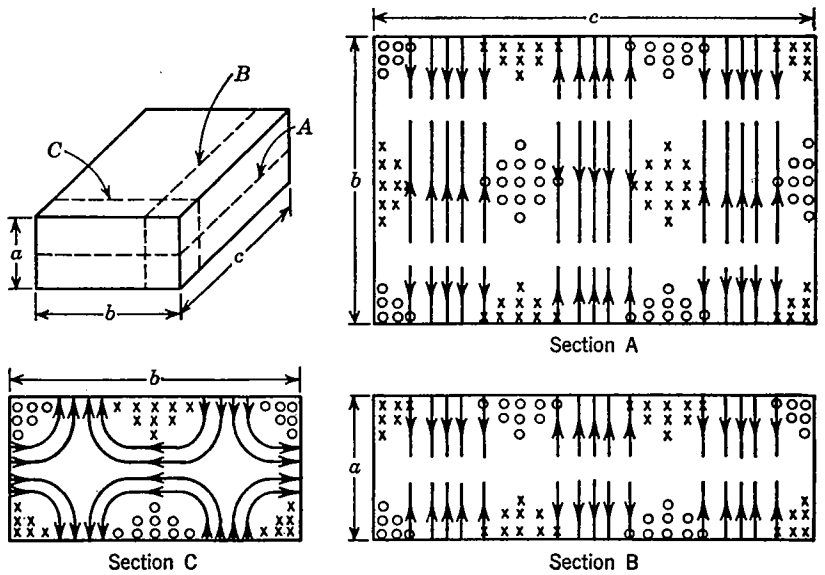

FIG. 4-5. Rectangular cavity mode pattern for the TE_{123} mode.

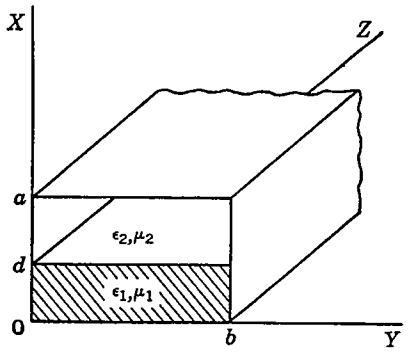

FIG. 4-6. A partially dielectric-filled rectangular waveguide.

stored in the dielectric and the losses are dissipated in the conducting walls.

4-6. Partially Filled Waveguide.[1] Consider a waveguide that is dielectric filled between $x = 0$ and $x = d$ (or has two dielectrics). This is illustrated by Fig. 4-6. The problem contains two homogeneous regions, $0 < x < d$ and $d < x < a$. Such problems are solved by finding solutions in each region such that tangential components of **E** and **H** are continuous across the common boundary. An attempt to find modes either TE to z or TM to z will prove unsuccessful, except for the TE_{m0} case. Most modes are therefore hybrid, having both E_z and H_z. An attempt to find modes TE or TM to x will prove successful, as we now show.

For fields TM to x, we choose ψ's in each region (region 1 is $x < d$, region 2 is $x > d$) to represent the x component of **A**, as in Eq. (4-29). The field in terms of the ψ's is then given by Eqs. (4-30). To satisfy the boundary conditions at the conducting walls, we take

$$\begin{aligned} \psi_1 &= C_1 \cos k_{x1}x \sin \frac{n\pi y}{b} e^{-jk_z z} \\ \psi_2 &= C_2 \cos [k_{x2}(a - x)] \sin \frac{n\pi y}{b} e^{-jk_z z} \end{aligned} \tag{4-41}$$

with $n = 1, 2, 3, \ldots$. It has been anticipated that $k_y = n\pi/b$ and k_z must be the same in each region for matching tangential **E** and **H** at $x = d$. The separation parameter equations in the two regions are

$$\begin{aligned} k_{x1}^2 + \left(\frac{n\pi}{b}\right)^2 + k_z^2 &= k_1^2 = \omega^2\epsilon_1\mu_1 \\ k_{x2}^2 + \left(\frac{n\pi}{b}\right)^2 + k_z^2 &= k_2^2 = \omega^2\epsilon_2\mu_2 \end{aligned} \tag{4-42}$$

[1] L. Pincherle, Electromagnetic Waves in Metal Tubes Filled Longitudinally with Two Dielectrics, *Phys. Rev.*, vol. 66, no. 5, pp. 118–130, 1944.

From Eqs. (4-30) and (4-41) we calculate

$$\begin{aligned} E_{y1} &= -\frac{1}{j\omega\epsilon_1} C_1 k_{x1} \frac{n\pi}{b} \sin k_{x1}x \cos \frac{n\pi y}{b} e^{-jk_z z} \\ E_{y2} &= \frac{1}{j\omega\epsilon_2} C_2 k_{x2} \frac{n\pi}{b} \sin [k_{x2}(a - x)] \cos \frac{n\pi y}{b} e^{-jk_z z} \\ E_{x1} &= \frac{1}{\omega\epsilon_1} C_1 k_{x1} k_z \sin k_{x1}x \sin \frac{n\pi y}{b} e^{-jk_z z} \\ E_{x2} &= -\frac{1}{\omega\epsilon_2} C_2 k_{x2} k_z \sin [k_{x2}(a - x)] \sin \frac{n\pi y}{b} e^{-jk_z z} \end{aligned}$$

Continuity of E_y and E_z at $x = d$ requires that

$$\frac{1}{\epsilon_1} C_1 k_{x1} \sin k_{x1}d = -\frac{1}{\epsilon_2} C_2 k_{x2} \sin [k_{x2}(a - d)] \tag{4-43}$$

Similarly, from Eqs. (4-30) and (4-41) we calculate

$$\begin{aligned} H_{y1} &= -jk_z C_1 \cos k_{x1}x \sin \frac{n\pi y}{b} e^{-jk_z z} \\ H_{y2} &= -jk_z C_2 \cos [k_{x2}(a - x)] \sin \frac{n\pi y}{b} e^{-jk_z z} \\ H_{x1} &= \frac{n\pi}{b} C_1 \cos k_{x1}x \cos \frac{n\pi y}{b} e^{-jk_z z} \\ H_{x2} &= \frac{n\pi}{b} C_2 \cos [k_{x2}(a - x)] \cos \frac{n\pi y}{b} e^{-jk_z z} \end{aligned}$$

Continuity of H_y and H_z at $x = d$ requires that

$$C_1 \cos k_{x1}d = C_2 \cos [k_{x2}(a - d)] \tag{4-44}$$

Division of Eq. (4-43) by Eq. (4-44) gives

$$\frac{k_{x1}}{\epsilon_1} \tan k_{x1}d = -\frac{k_{x2}}{\epsilon_2} \tan [k_{x2}(a - d)] \tag{4-45}$$

Both k_{x1} and k_{x2} are functions of k_z by Eqs. (4-42); so the above is a transcendental equation for determining possible k_z's (mode-propagation constants). Once the desired k_z is found, k_{x1} and k_{x2} are given by Eqs. (4-42), and the ratio C_2/C_1 is given by Eq. (4-43) or Eq. (4-44).

For fields TE to x, we choose ψ's in each region to represent the x component of **F**. To satisfy the boundary conditions at the conducting walls, we take

$$\begin{aligned} \psi_1 &= C_1 \sin k_{x1}x \cos \frac{n\pi y}{b} e^{-jk_z z} \\ \psi_2 &= C_2 \sin [k_{x2}(a - x)] \cos \frac{n\pi y}{b} e^{-jk_z z} \end{aligned} \tag{4-46}$$

with $n = 0, 1, 2, \ldots$. The separation parameter equations are again Eqs. (4-42). The field is calculated from the ψ's by Eqs. (4-32). A matching of tangential **E** and **H** at $x = d$ yields the characteristic equation

$$\frac{k_{x1}}{\mu_1} \cot k_{x1}d = -\frac{k_{x2}}{\mu_2} \cot [k_{x2}(a - d)] \tag{4-47}$$

The k_{x1} and k_{x2} are functions of k_z by Eqs. (4-42); so the above is a transcendental equation for determining k_z's for the modes TE to x.

The modes of the partially filled rectangular waveguide are distorted versions of the TEx and TMx modes of Sec. 4-4. The mode patterns are similar to those of Fig. 4-4, except that the field tends to concentrate in the material of higher ϵ and μ. In the lossless case, the cutoff frequencies ($k_z = 0$) of the various modes will always lie between those for the corresponding modes of a guide filled with a material ϵ_1, μ_1, and those of a guide filled with a material ϵ_2, μ_2. (This can be shown by the perturbational procedure of Sec. 7-4.) In contrast to the filled guide, the cutoff frequencies of the corresponding TEx and TMx modes will be different. Also, a knowledge of the cutoff frequencies of the partially filled guide is *not* sufficient to determine k_z at other frequencies by Eq. (4-26). We have to solve Eqs. (4-45) and (4-47) at each frequency.

Of special interest is the dominant mode of a partially filled guide. For $b > a$, this is the mode corresponding to the TMx_{01} mode of the empty guide, which is also the TE$_{01}$ mode of the empty guide. For a given n, Eq. (4-45) has a denumerably infinite set of solutions. We shall let m denote the order of these solutions, as follows. The mode with the lowest cutoff frequency is denoted by $m = 0$, the next mode by $m = 1$, and so on. This numbering system is chosen so that the TMx_{mn} partially filled waveguide modes correspond to the TMx_{mn} empty-guide modes. The dominant mode of the partially filled guide is then the TMx_{01} mode when $b > a$. Hence, the propagation constant of the dominant mode is given by the lowest-order solution to Eq. (4-45) when the k_x's are given by Eqs. (4-42) with $n = 1$. Figure 4-7 shows some calculations for the case $\epsilon = 2.45\epsilon_0$.

When k_1 is not very different from k_2, we should expect k_{x1} and k_{x2} to be small (k_x is zero in an empty guide). If this is so, then Eq. (4-45) can be approximated by

$$\frac{k_{x1}^2 d}{\epsilon_1} \approx \frac{-k_{x2}^2(a - d)}{\epsilon_2} \tag{4-48}$$

With this explicit relationship between k_{x1} and k_{x2}, we can solve Eqs. (4-42) simultaneously for k_{x1} and k_z (given ω). Note that when k_{x1} is real, k_{x2} is imaginary, and vice versa. The cutoff frequency is obtained by setting $k_z = 0$ in Eqs. (4-42). Using Eq. (4-48), we have for the

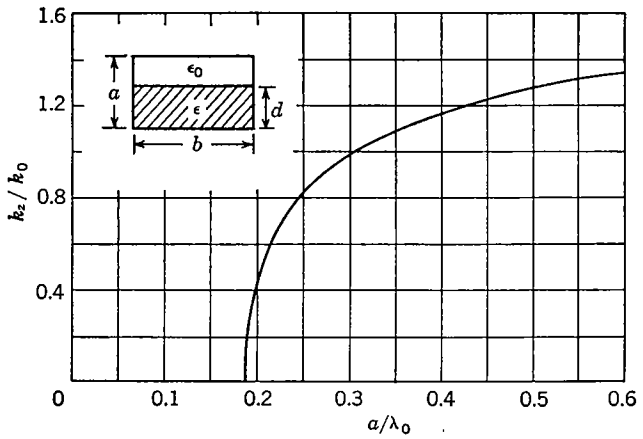

FIG. 4-7. Propagation constant for a rectangular waveguide partially filled with dielectric, $\epsilon = 2.45\epsilon_0$, $a/b = 0.45$, $d/a = 0.50$. (*After Frank.*)

dominant mode

$$k_{x1}^2 + \left(\frac{\pi}{b}\right)^2 = \omega^2\epsilon_1\mu_1$$

$$\frac{-\epsilon_2 d}{\epsilon_1(a - d)} k_{x1}^2 + \left(\frac{\pi}{b}\right)^2 = \omega^2\epsilon_2\mu_2$$

These we solve for the cutoff frequency $\omega = \omega_c$, obtaining

$$\omega_c \approx \frac{\pi}{b} \sqrt{\frac{\epsilon_1(a - d) + \epsilon_2 d}{\epsilon_1(a - d)\epsilon_2\mu_2 + \epsilon_2 d\epsilon_1\mu_1}} \tag{4-49}$$

valid when Eq. (4-48) applies. When $\mu_1 = \mu_2 = \mu$, this reduces to

$$\omega_c \approx \frac{\pi}{b} \sqrt{\frac{\epsilon_1(a - d) + \epsilon_2 d}{\mu\epsilon_1\epsilon_2 a}} \tag{4-50}$$

Note that this is the equation for resonance of a parallel-plate transmission line, shorted at each end, and having

$$L = \mu a \qquad C = \frac{\epsilon_1\epsilon_2}{\epsilon_1(a - d) + \epsilon_2 d}$$

per unit width. All cylindrical (cross section independent of z) waveguides at cutoff are two-dimensional resonators.

A waveguide partially filled in the opposite manner (dielectric boundary parallel to the narrow side of the guide) is the same problem with $a > b$. The dominant mode of the empty guide is then the TEx_{10} mode, or TE$_{10}$ mode. The dominant mode of the partially filled guide will also be a

TEx mode; so the eigenvalues are found from Eq. (4-47) with $n = 0$. We shall order the modes by m as follows. That with the lowest cutoff frequency is denoted by $m = 1$, that with the next lowest by $m = 2$, and so on. This numbering system corresponds to that for the empty guide, the dominant mode being the TEx_{10} mode. When k_1 is not too different from k_2, we might expect k_{x1} and k_{x2} to be close to the empty-guide value $k_x = \pi/a$. An approximate solution to Eq. (4-47) could then be found by perturbing k_{x1} and k_{x2} about π/a. For the cutoff frequency of the

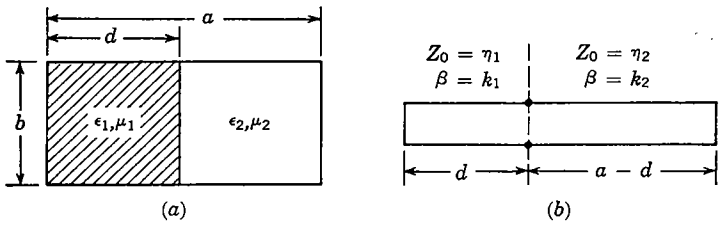

FIG. 4-8. (*a*) Partially filled waveguide; (*b*) transmission-line resonator. The cutoff frequency of the dominant mode of (*a*) is the resonant frequency of (*b*).

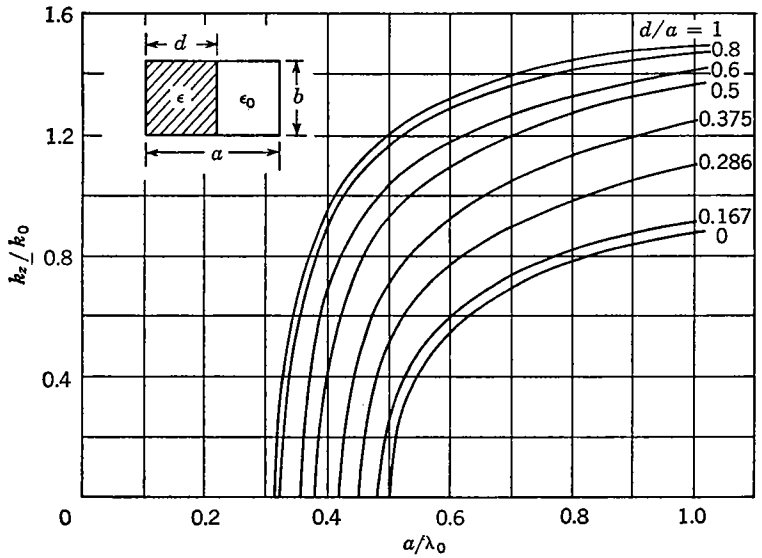

FIG. 4-9. Propagation constant for a rectangular waveguide partially filled with dielectric, $\epsilon = 2.45\epsilon_0$. (*After Frank.*)

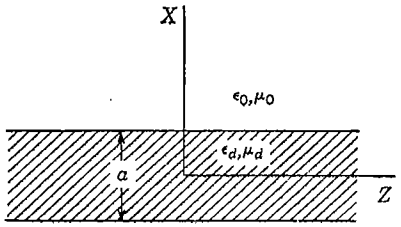

FIG. 4-10. The dielectric-slab waveguide.

dominant mode, Eqs. (4-42) become

$$k_{x1}^2 = k_{1c}^2 = \omega_c^2\epsilon_1\mu_1$$
$$k_{x2}^2 = k_{2c}^2 = \omega_c^2\epsilon_2\mu_2$$

and Eq. (4-47) becomes

$$\frac{1}{\eta_1}\cot k_{1c}d = -\frac{1}{\eta_2}\cot\left[k_{2c}(a-d)\right] \tag{4-51}$$

It is interesting to note that this is the equation for resonance of two short-circuited transmission lines having Z_0's of η_1 and η_2, and β's of k_{1c} and k_{2c}, as illustrated by Fig. 4-8. The reason for this is, at cutoff, the TEx_{10} mode reduces to the parallel-plate transmission-line mode that propagates in the x direction. This viewpoint has been used extensively by Frank.[1]

Some calculated propagation constants for the dominant mode are shown in Fig. 4-9 for the case $\epsilon = 2.45\epsilon_0$. Similar results for a centered dielectric slab are shown in Fig. 7-10, and the characteristic equation for that case is given in Prob. 4-19.

4-7. The Dielectric-slab Guide. It is not necessary to have conductors for the guidance or localization of waves. Such phenomena also occur in inhomogeneous dielectrics. The simplest illustration of this is the guidance of waves by a dielectric slab. The so-called slab waveguide is illustrated by Fig. 4-10.

We shall consider the problem to be two-dimensional, allowing no variation with the y coordinate. It is desired to find z-traveling waves, that is, $e^{-jk_z z}$ variation. Modes TE and TM to either x or z can be found, and we shall choose the latter representation. For modes TM to z, Eqs. (3-86) reduce to

$$E_x = \frac{-k_z}{\omega\epsilon}\frac{\partial\psi}{\partial x} \qquad E_z = \frac{1}{j\omega\epsilon}(k^2 - k_z^2)\psi \qquad H_y = -\frac{\partial\psi}{\partial x} \tag{4-52}$$

We shall consider separately the two cases: (1) ψ an odd function of x, denoted by ψ^o, and (2) ψ an even function of x, denoted by ψ^e. For case

[1] N. H. Frank, Wave Guide Handbook, *MIT Rad. Lab. Rept.* 9, 1942.

(1), we choose in the dielectric region

$$\psi_d^o = A \sin ux\, e^{-jk_z z} \qquad |x| < \frac{a}{2} \tag{4-53}$$

and in the air region

$$\begin{aligned} \psi_a^o &= Be^{-vx}e^{-jk_z z} && x > \frac{a}{2} \\ \psi_a^o &= -Be^{vx}e^{-jk_z z} && x < -\frac{a}{2} \end{aligned} \tag{4-54}$$

We have chosen $k_{xd} = u$ and $k_{x0} = jv$ for simplicity of notation. (It will be seen later that u and v are real for unattenuated wave propagation.) The separation parameter equations in each region become

$$\begin{aligned} u^2 + k_z^2 &= k_d^2 = \omega^2\epsilon_d\mu_d \\ -v^2 + k_z^2 &= k_0^2 = \omega^2\epsilon_0\mu_0 \end{aligned} \tag{4-55}$$

Evaluating the field components tangential to the air-dielectric interface, we have

$$\left.\begin{aligned} E_z &= \frac{A}{j\omega\epsilon_d} u^2 \sin ux\, e^{-jk_z z} \\ H_y &= -Au \cos ux\, e^{-jk_z z} \end{aligned}\right\} \qquad |x| < \frac{a}{2}$$

$$H_y = Bve^{-v|x|}e^{-jk_z z} \qquad |x| > \frac{a}{2}$$

$$E_z = \frac{-B}{j\omega\epsilon_0} v^2 e^{-vx}e^{-jk_z z} \qquad x > \frac{a}{2}$$

$$E_z = \frac{B}{j\omega\epsilon_0} v^2 e^{vx}e^{-jk_z z} \qquad x < -\frac{a}{2}$$

Continuity of E_z and H_y at $x = \pm a/2$ requires that

$$\begin{aligned} \frac{A}{\epsilon_d} u^2 \sin \frac{ua}{2} &= \frac{-B}{\epsilon_0} v^2 e^{-va/2} \\ Au \cos \frac{ua}{2} &= -Bve^{-va/2} \end{aligned}$$

The ratio of the first equation to the second gives

$$\frac{ua}{2} \tan \frac{ua}{2} = \frac{\epsilon_d}{\epsilon_0} \frac{va}{2} \tag{4-56}$$

This, coupled with Eqs. (4-55), is the characteristic equation for determining k_z's and cutoff frequencies of the odd TM modes.

For TM modes which are even functions of x, we choose

$$\begin{aligned} \psi_d^e &= A \cos ux\, e^{-jk_z z} && |x| < \frac{a}{2} \\ \psi_a^e &= Be^{-v|x|}e^{-jk_z z} && |x| > \frac{a}{2} \end{aligned} \tag{4-57}$$

The separation parameter equations are still Eqs. (4-55). The field components are still given by Eqs. (4-52). In this case, matching E_z and H_y at $x = \pm a/2$ yields

$$-\frac{ua}{2} \cot \frac{ua}{2} = \frac{\epsilon_d}{\epsilon_0} \frac{va}{2} \tag{4-58}$$

This is the characteristic equation for determining the k_z's and cutoff frequencies of the even TM modes.

There is complete duality between the TM and TE modes of the slab waveguide; so the characteristic equations must be dual. For the TE modes with odd ψ we have

$$\frac{ua}{2} \tan \frac{ua}{2} = \frac{\mu_d}{\mu_0} \frac{va}{2} \tag{4-59}$$

as the characteristic equation, and for the TE modes with even ψ we have

$$-\frac{ua}{2} \cot \frac{ua}{2} = \frac{\mu_d}{\mu_0} \frac{va}{2} \tag{4-60}$$

as the characteristic equation. The u's and v's still satisfy Eqs. (4-55). The odd wave functions generating the TE modes are those of Eqs. (4-53) and (4-54), and the even wave functions generating the TE modes are those of Eqs. (4-57). The fields are, of course, obtained from the ψ's by equations dual to Eqs. (4-52), which are, explicitly,

$$H_x = -\frac{k_z}{\omega\mu} \frac{\partial\psi}{\partial x} \qquad H_z = \frac{1}{j\omega\mu} (k^2 - k_z^2)\psi \qquad E_y = \frac{\partial\psi}{\partial x} \tag{4-61}$$

These are specializations of Eqs. (3-89).

The concept of cutoff frequency for dielectric waveguides is given a somewhat different interpretation than for metal guides. Above the cutoff frequency, as we define it, the dielectric guide propagates a mode unattenuated (k_z is real). Below the cutoff frequency, there is attenuated propagation ($k_z = \beta - j\alpha$). Since the dielectric is loss free, this attenuation must be accounted for by radiation of energy as the wave progresses. Dielectric guides operated in a radiating mode (below cutoff) are used as antennas. The phase constant of an unattenuated mode lies between the intrinsic phase constant of the dielectric and that of air; that is,

$$k_0 < k_z < k_d$$

This can be shown as follows. Equations (4-55) require that u and v be either real or imaginary when k_z is real. The characteristic equations have solutions only when v is real. Furthermore, v must be positive, else the field will increase with distance from the slab [see Eqs. (4-54) or (4-57)]. When v is real and positive the characteristic equations have solutions only when u is also real. Hence, both u and v are real, and it follows from Eqs. (4-55) that $k_0 < k_z < k_d$. This result is a property of cylindrical dielectric waveguides in general.

The lowest frequency for which unattenuated propagation exists is called the *cutoff frequency*. From the above discussion, it is evident that cutoff occurs as $k_z \to k_0$, in which case $v \to 0$. The cutoff frequencies are therefore obtained from the characteristic equations by setting $u = \sqrt{k_d^2 - k_0^2}$ and $v = 0$. The result is

$$\tan\left(\frac{a}{2}\sqrt{k_d^2 - k_0^2}\right) = 0 \qquad \cot\left(\frac{a}{2}\sqrt{k_d^2 - k_0^2}\right) = 0$$

which apply to both TE and TM modes. These equations are satisfied when

$$\frac{a}{2}\sqrt{k_d^2 - k_0^2} = \frac{n\pi}{2} \qquad n = 0, 1, 2, \ldots$$

This we solve for the cutoff wavelengths

$$\lambda_c = \frac{2a}{n}\sqrt{\frac{\epsilon_d\mu_d}{\epsilon_0\mu_0} - 1} \qquad n = 0, 1, 2, \ldots \tag{4-62}$$

and the cutoff frequencies

$$f_c = \frac{n}{2a\sqrt{\epsilon_d\mu_d - \epsilon_0\mu_0}} \qquad n = 0, 1, 2, \ldots \tag{4-63}$$

The modes are ordered as TM_n and TE_n according to the choice of n in Eqs. (4-62) and (4-63). Note that f_c for the TE_0 and TM_0 modes is zero. In other words, *the lowest-order TE and TM modes propagate unattenuated no matter how thin the slab.* This is a general property of cylindrical dielectric waveguides; the cutoff frequency of the dominant mode (or modes) is zero. However, as the slab becomes very thin, $k_z \to k_0$ and $v \to 0$, so the field extends great distances from the slab. This characteristic is considered further in the next section. Finally, observe from Eq. (4-62) that when $\epsilon_d\mu_d \gg \epsilon_0\mu_0$, the cutoffs occur when the guide width is approximately an integral number of half-wavelengths *in the dielectric*, zero half-wavelength included.

Simple graphical solutions of the characteristic equations exist to determine k_z at any frequency above cutoff. Let us demonstrate this

for the TE modes. Elimination of k_z from Eqs. (4-55) gives

$$u^2 + v^2 = k_d^2 - k_0^2 = \omega^2(\epsilon_d\mu_d - \epsilon_0\mu_0)$$

Using this relationship, we can write the TE characteristic equations as

$$\left.\begin{aligned} &\frac{\mu_0}{\mu_d}\frac{ua}{2}\tan\frac{ua}{2} \\ &-\frac{\mu_0}{\mu_d}\frac{ua}{2}\cot\frac{ua}{2} \end{aligned}\right\} = \sqrt{\left(\frac{\omega a}{2}\right)^2(\epsilon_d\mu_d - \epsilon_0\mu_0) - \left(\frac{ua}{2}\right)^2}$$

Values of $ua/2$ for the various modes are the intersections of the plot of the left-hand terms with the circle specified by the right-hand term. Figure 4-11 shows a plot of the left-hand terms for $\mu_d = \mu_0$. A representative plot of the right-hand term is shown dashed. As ω or ϵ_d is varied, only the radius of the circle changes. (For the case shown, only three TE modes are above cutoff.) If $\mu_d \neq \mu_0$, the solid curves must be redrawn. The graphical solution for the TM mode eigenvalues is similar.

Sketches of the mode patterns are also of interest. Figure 4-12 shows the patterns of the TE_0 and TM_1 modes. These can also be interpreted as the mode patterns of the TM_0 and TE_1 modes if $\mathcal{E}$ and $\mathcal{H}$ are interchanged, for there is complete duality between the TE and TM cases.

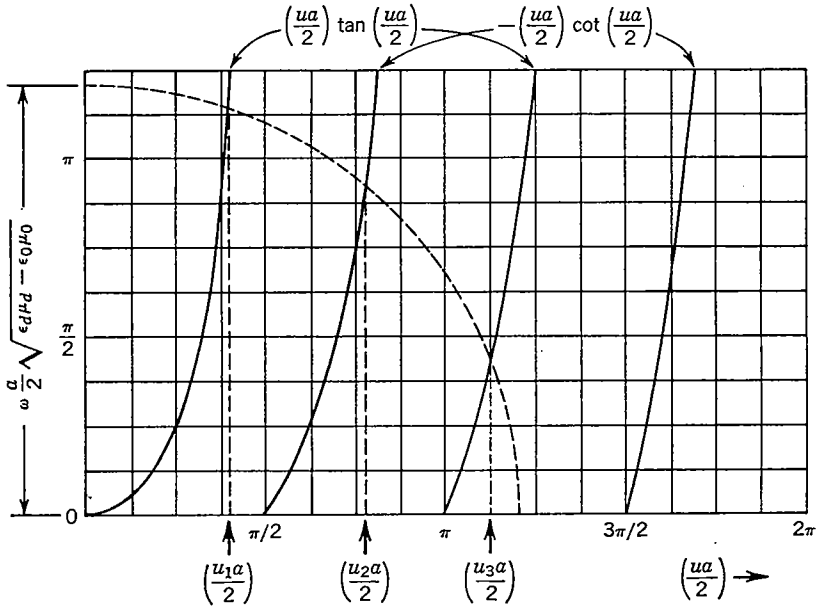

FIG. 4-11. Graphical solution of the characteristic equation for the slab waveguide.

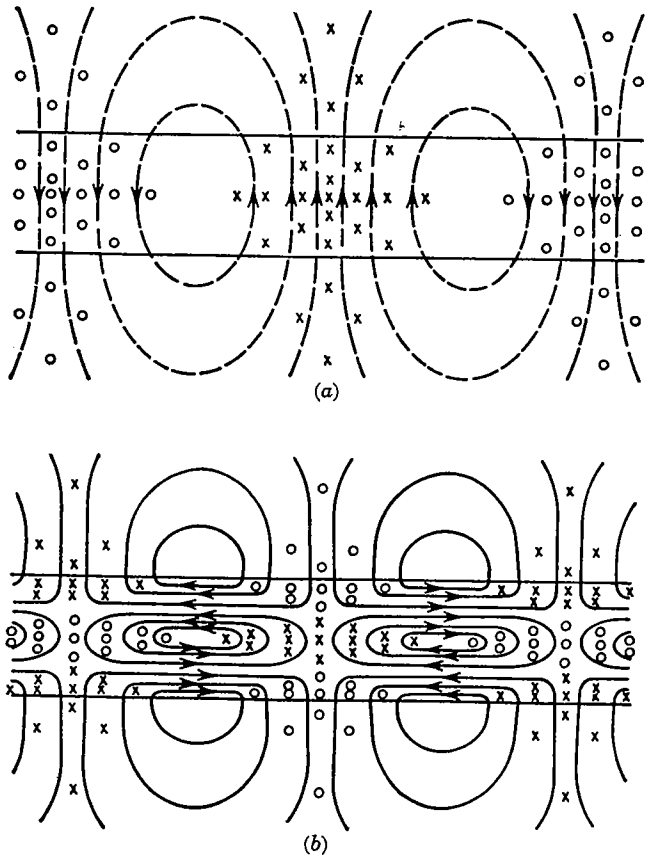

FIG. 4-12. Mode patterns for the dielectric-slab waveguide. (*a*) TE_0 mode ($\mathcal{H}$ lines dashed); (*b*) TM_1 mode ($\mathcal{E}$ lines solid).

As the mode number increases, more loops appear within the dielectric, but not in the air region.

4-8. Surface-guided Waves. We shall show that any "reactive boundary" will tend to produce wave guidance along that boundary. The wave impedances normal to the dielectric-to-air interfaces of the slab guide of Fig. 4-10 can be shown to be reactive. A simple way of obtaining a single reactive surface is to coat a conductor with a dielectric layer. This is shown in Fig. 4-13.

The modes of the dielectric-coated conductor are those of the dielectric slab having zero tangential **E** over the $x = 0$ plane. These are the TM_n, $n = 0, 2, 4, \ldots$, modes (odd ψ) and the TE_n, $n = 1, 3, 5, \ldots$, modes

(even ψ) of the slab. We shall retain the same mode designations for the coated conductor. The characteristic equations for the TM modes of the coated conductor are therefore Eq. (4-56) with $a/2$ replaced by t (coating thickness). The characteristic equation for the TE modes is Eq. (4-60) with $a/2$ replaced by t. The cutoff frequencies are specified by Eq. (4-63), which, for the coated conductor, becomes

$$f_c = \frac{n}{4t\sqrt{\epsilon_d\mu_d - \epsilon_0\mu_0}} \tag{4-64}$$

where for TM modes $n = 0, 2, 4, \ldots$, and for TE modes $n = 1, 3, 5, \ldots$. The dominant mode is the TM_0 mode, which propagates unattenuated at all frequencies. The mode pattern of the TM_0 mode is sketched in Fig. 4-14.

Let us consider in more detail the manner in which the dominant mode decays with distance from the boundary. In the air space, the field attenuates as e^{-vx}. For thick coatings, $k_z \to k_d$, and, from Eq. (4-55),

$$v \xrightarrow[t\ \text{large}]{} k_0\sqrt{\frac{\epsilon_d\mu_d}{\epsilon_0\mu_0} - 1} \tag{4-65}$$

This attenuation is quite large for most dielectrics. For example, if the coating is polystyrene ($\epsilon_d = 2.56\epsilon_0$, $\mu_d = \mu_0$), the field in 0.12λ has decayed to 36.8 per cent of its value at the surface. However, for thin coatings,

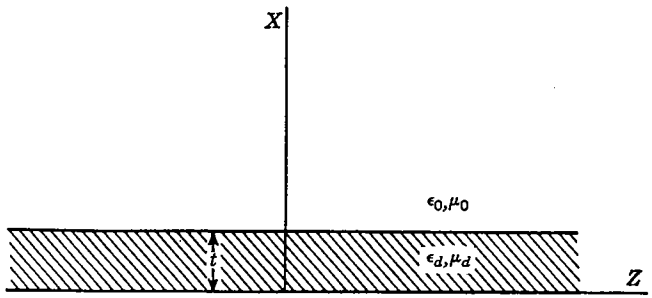

FIG. 4-13. A dielectric-coated conductor.

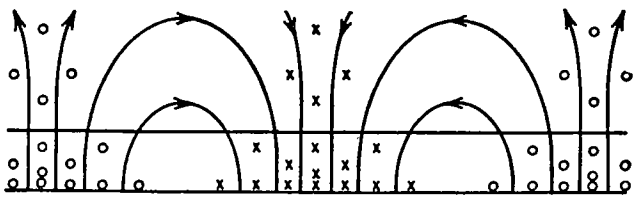

FIG. 4-14. The TM_0 mode pattern for the coated conductor ($\mathcal{E}$ lines solid.)

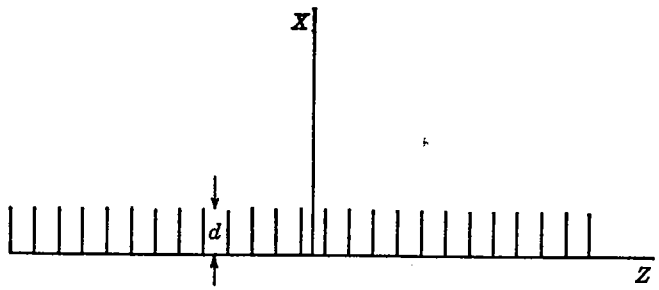

FIG. 4-15. A corrugated conductor.

the field decays slowly. In this case, $k_z \to k_0$, and

$$v \xrightarrow[t \text{ small}]{} 2\pi k_0 \left(\frac{\mu_d}{\mu_0} - \frac{\epsilon_0}{\epsilon_d}\right)\frac{t}{\lambda} \tag{4-66}$$

If the polystyrene coating were 0.0001 wavelength thick, we would have to go 40 wavelengths from the surface before the field decays to 36.8 per cent of its value at the surface. We say that the field is "tightly bound" to a thick dielectric coating and "loosely bound" to a thin dielectric coating.

Another way of obtaining a reactive surface is to "corrugate" a conducting surface, as suggested by Fig. 4-15. For a simple treatment of the problem, let us assume that the "teeth" are infinitely thin, and that there are many slots per wavelength. The teeth will essentially short out any E_y, permitting only E_z and E_x at the surface. The TM fields of the dielectric-slab guide are of this type; hence we shall assume that this field exists in the air region. Extracting from Sec. 4-7, we have

$$\left.\begin{aligned} E_x &= \frac{k_z}{\omega\epsilon_0} H_y \\ E_z &= \frac{-B}{j\omega\epsilon_0} v^2 e^{-vx} e^{-jk_z z} \\ H_y &= Bve^{-vx}e^{-jk_z z} \end{aligned}\right\} \quad x > d$$

where
$$-v^2 + k_z^2 = k_0^2 = \omega^2\epsilon_0\mu_0 \tag{4-67}$$

The wave impedance looking into the corrugated surface is

$$Z_{-x} = \frac{E_z}{H_y} = \frac{jv}{\omega\epsilon_0} \tag{4-68}$$

Note that this is inductively reactive; so to support such a field, the interface must be an inductively reactive surface. (The TE fields of Sec. 4-7 require a capacitively reactive surface.) In the slots of the corrugation, we assume that the parallel-plate transmission-line mode

exists. These are then short-circuited transmission lines, of characteristic wave impedance η_0. Hence, the input wave impedance is

$$Z_{-x} = j\eta_0 \tan k_0 d \tag{4-69}$$

For $k_0 d < \pi/2$, this is inductively reactive. Equating Eqs. (4-68) and (4-69), we have

$$v = k_0 \tan k_0 d \tag{4-70}$$

and, from Eq. (4-67), we have

$$k_z = k_0\sqrt{1 + \tan^2 k_0 d} \tag{4-71}$$

It should be pointed out that this solution is approximate, for we have only approximated the wave impedance at $x = d$. In the true solution, the fields must differ from those assumed in the vicinity of $x = d$. (We should expect E_x to terminate on the edges of the teeth.)

When the teeth are considered to be of finite width, an approximate solution can be obtained by replacing Eq. (4-69) by the average wave impedance. This is found by assuming Eq. (4-69) to hold over the gaps, and by assuming zero impedance over the region occupied by the teeth. The result is[1]

$$k_z \approx k_0\sqrt{1 + \left(\frac{g}{g+t}\right)^2 \tan^2 k_0 d}$$

where g = width of gaps and t = width of teeth.

While at this time we lack the concepts for estimating the accuracy of the above solution, it has been found to be satisfactory for small $k_0 d$. Note that, from Eq. (4-70), the wave is loosely bound for very small $k_0 d$, becoming more tightly bound as $k_0 d$ becomes larger (but still less than $\pi/2$). The mode pattern of the wave is similar to that for the TM_0 coated-conductor mode (Fig. 4-14), except in the vicinity of the corrugations.

4-9. Modal Expansions of Fields. The modes existing in a waveguide depend upon the excitation of the guide. The nonpropagating modes are of appreciable magnitude only in the vicinity of sources or discontinuities. Given the tangential components of **E** (or of **H**) over a waveguide cross section, we can determine the amplitudes of the various waveguide modes. This we shall illustrate for the rectangular waveguide.

Consider the rectangular waveguide of Fig. 2-16. Let $E_x = 0$ and $E_y = f(x,y)$ be known over the $z = 0$ cross section. We wish to determine the field $z > 0$, assuming that the guide is matched (only outward-traveling waves exist). The TEx modes of Sec. 4-4 have no E_x; so let us

[1] C. C. Cutler, Electromagnetic Waves Guided by Corrugated Conducting Surfaces, *Bell Telephone Lab. Rept.* MM-44-160-218, October, 1944.

take a superposition of these modes. This is

$$\psi = \sum_{m=1}^{\infty} \sum_{n=0}^{\infty} A_{mn} \sin \frac{m\pi x}{a} \cos \frac{n\pi y}{b} e^{-\gamma_{mn} z} \tag{4-72}$$

where A_{mn} are mode amplitudes and the γ_{mn} are the mode-propagation constants, given by Eq. (4-23). In terms of ψ, the field is given by Eqs. (4-32). In particular, E_y at $z = 0$ is given by

$$E_y\Big|_{z=0} = \sum_{m=1}^{\infty} \sum_{n=0}^{\infty} \gamma_{mn} A_{mn} \sin \frac{m\pi x}{a} \cos \frac{n\pi y}{b}$$

Note that this is in the form of a double Fourier series: a sine series in x and a cosine series in y (see Appendix C). It is thus evident that $\gamma_{mn} A_{mn}$ are the Fourier coefficients of E_y, or

$$\gamma_{mn} A_{mn} = E_{mn} = \frac{2\epsilon_n}{ab} \int_0^a dx \int_0^b dy\, E_y\Big|_{z=0} \sin \frac{m\pi x}{a} \cos \frac{n\pi y}{b} \tag{4-73}$$

where $\epsilon_n = 1$ for $n = 0$ and $\epsilon_n = 2$ for $n > 0$ (*Neumann's number*). The A_{mn}, and hence the field, are now evaluated. The solution for $E_x = f(x,y)$ and $E_y = 0$ given over the $z = 0$ cross section can be obtained from the above solution by a rotation of axes. The general case for which both E_x and E_y are given over the $z = 0$ cross section is a superposition of the two cases $E_x = 0$ and $E_y = 0$. The solution for the case H_x and H_y given over the $z = 0$ cross section can be obtained in a dual manner.

For a large class of waveguides, when many modes exist simultaneously, each mode transmits energy as if it existed alone. We shall show that the rectangular waveguide has this property. Given the wave function of Eq. (4-72), specifying a field according to Eqs. (4-32), the z-directed complex power at $z = 0$ is

$$\begin{aligned} P &= \iint_{z=0} \mathbf{E} \times \mathbf{H}^* \cdot \mathbf{u}_z\, ds = -\int_0^a dx \int_0^b dy\, [E_y H_x^*]_{z=0} \\ &= \int_0^a dx \int_0^b dy \left[\sum_{m,n} E_{mn} \sin \frac{m\pi x}{a} \cos \frac{n\pi y}{b} \right] \\ &\qquad \times \left[\sum_{p,q} \frac{k^2 - \left(\frac{p\pi}{a}\right)^2}{j\omega\mu\gamma_{pq}^*} E_{pq}^* \sin \frac{p\pi x}{a} \cos \frac{q\pi y}{b} \right] \end{aligned}$$

Because of the orthogonality relationships for the sinusoidal functions,

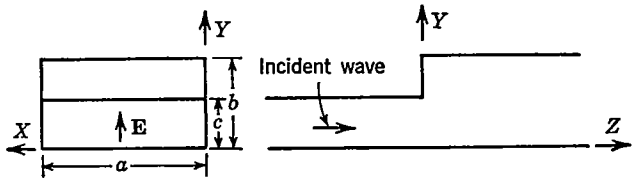

FIG. 4-16. A capacitive waveguide junction.

this reduces to

$$P = \sum_{m=1}^{\infty} \sum_{n=0}^{\infty} (Y_0)_{mn}^* |E_{mn}|^2 \frac{ab}{2\epsilon_n} \tag{4-74}$$

where $(Y_0)_{mn}$ are the TEx wave admittances, given by the reciprocal of Eqs. (4-36). The above equation is simply a summation of the powers for the individual modes. In a lossless guide, the power for a propagating mode is real and that for a nonpropagating mode is imaginary.

To illustrate the above theory, consider the waveguide junction of Fig. 4-16. The dimensions are such that only the dominant mode (TE_{10}) propagates in each section. Let there be a wave incident on the junction from the smaller guide, and let the larger guide be matched. For an approximate solution, assume that E_y at the junction is that of the incident wave

$$E_y\Big|_{z=0} \approx \begin{cases} \sin \dfrac{\pi x}{a} & y < c \\ 0 & y > c \end{cases} \tag{4-75}$$

From Eq. (4-73), the only nonzero mode amplitudes are

$$\begin{aligned} E_{10} &= \gamma_{10} A_{10} = \frac{c}{b} \\ E_{1n} &= \gamma_{1n} A_{1n} = \frac{2}{n\pi} \sin \frac{n\pi c}{b} \end{aligned} \tag{4-76}$$

Thus, only the $m = 1$ term of the m summation remains in Eq. (4-72).

Let us use this solution to obtain an "aperture admittance" for the junction. From Eqs. (4-74) and (4-76), the complex power at $z = 0$ is

$$P = \frac{ac^2}{2b} \left\{ (Y_0)_{10}^* + 2 \sum_{n=1}^{\infty} (Y_0)_{1n}^* \left[\frac{\sin (n\pi c/b)}{n\pi c/b} \right]^2 \right\}$$

where, from Eqs. (4-36),

$$\begin{aligned} (Y_0)_{10} &= \frac{k^2 - (\pi/a)^2}{\omega\mu\beta} = \frac{\sqrt{1 - (f_c/f)^2}}{\eta} \\ (Y_0)_{1n} &= \frac{k^2 - (\pi/a)^2}{-j\omega\mu\alpha} = \frac{j2b(Y_0)_{10}}{\lambda_g \sqrt{n^2 - (2b/\lambda_g)^2}} \end{aligned}$$

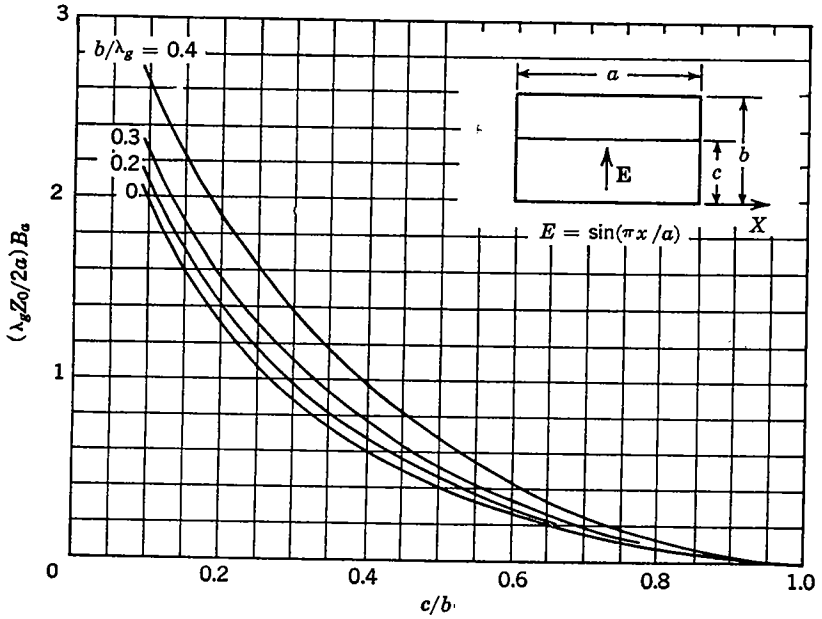

FIG. 4-17. Susceptance of a capacitive aperture.

The f_c and λ_g are those of the TE_{10} mode. We shall refer the aperture admittance to the voltage across the center of the aperture, which is $V = c$. The aperture admittance is then

$$Y_a = \frac{P^*}{|V|^2} = (Y_0)_{10}\left[\frac{a}{2b} + j\frac{2a}{\lambda_g}\sum_{n=1}^{\infty}\frac{\sin^2(n\pi c/b)}{(n\pi c/b)^2\sqrt{n^2 - (2b/\lambda_g)^2}}\right] \tag{4-77}$$

The imaginary part of this is the aperture susceptance

$$B_a = \frac{2a}{\lambda_g Z_0}\sum_{n=1}^{\infty}\frac{\sin^2(n\pi c/b)}{(n\pi c/b)^2\sqrt{n^2 - (2b/\lambda_g)^2}} \tag{4-78}$$

where λ_g and Z_0 are those of the dominant mode. Calculated values for B_a are shown in Fig. 4-17. For small c/b, we have[1]

$$\frac{\lambda_g Z_0}{2a}B_a \approx -\log\left\{0.656\,\frac{c}{b}\left[1 + \sqrt{1 - \left(\frac{2b}{\lambda_g}\right)^2}\right]\right\} \tag{4-79}$$

[1] This equation is a quasi-static result. The direct specialization of Eq. (4-78) to small c/b yields a numerical factor of 0.379 instead of 0.656.

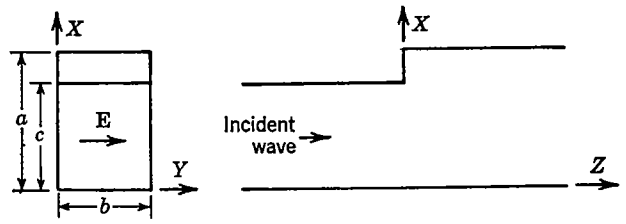

FIG. 4-18. An inductive waveguide junction.

The aperture susceptance is a quantity that will be useful for the treatment of microwave networks in Chap. 8. Note that the susceptance is capacitive (positive); so the original junction is called a *capacitive waveguide junction*. Remember that our solution is only approximate, since we assumed E in the aperture. (We shall see in Sec. 8-9 that the true susceptance cannot be greater than our present solution.) We have assumed that only one mode propagates in the guide; hence our solution is explicit only for

$$1 < \frac{f}{f_c} < \sqrt{1 + \left(\frac{a}{b}\right)^2}$$

When a second mode propagates, it contributes to the aperture conductance, and Eq. (4-78) would be summed from $n = 2$ to ∞, and so on.

Another problem of practical interest is that of the waveguide junction of Fig. 4-18. Again we assume only the dominant mode propagates in each section. Take a wave incident on the junction from the smaller guide, and let the larger guide be matched. For an approximate solution, we assume E_y in the aperture to be that of the incident wave

$$E_y|_{z=0} \approx \begin{cases} \sin\dfrac{\pi x}{c} & x < c \\ 0 & x > c \end{cases} \tag{4-80}$$

From Eqs. (4-73), we determine the only nonzero mode amplitudes as

$$E_{m0} = \frac{2c\sin(m\pi c/a)}{\pi a[1 - (mc/a)^2]} \tag{4-81}$$

Thus, only the $n = 0$ term of the n summation remains in Eq. (4-72).

Again we can find an aperture admittance for the junction. From Eqs. (4-74) and (4-81), the complex power at $z = 0$ is

$$P = \frac{2bc^2}{\pi^2 a}\sum_{m=1}^{\infty}(Y_0)_{m0}^*\left[\frac{\sin(m\pi c/a)}{1 - (mc/a)^2}\right]^2$$

where, from Eqs. (4-36),

$$(Y_0)_{10} = \frac{k^2}{\omega\mu\beta} = \frac{\sqrt{1 - (f_c/f)^2}}{\eta}$$

$$(Y_0)_{m0} = \frac{k^2 - (m\pi/a)^2}{-j\omega\mu\alpha} = \frac{-j}{\eta}\sqrt{\left(\frac{m\lambda}{2a}\right)^2 - 1} \qquad m > 1$$

The voltage across the center of the aperture is $V = b$. The aperture admittance referred to this voltage is therefore

$$Y_a = \frac{2c^2}{\pi^2 ab}\left\{\left[\frac{\sin(\pi c/a)}{1 - (c/a)^2}\right]^2 (Y_0)_{10} - \frac{j}{\eta}\sum_{m=2}^{\infty}\left[\frac{\sin(m\pi c/a)}{1 - (mc/a)^2}\right]^2 \sqrt{\left(\frac{m\lambda}{2a}\right)^2 - 1}\right\} \tag{4-82}$$

The imaginary part of this is the aperture susceptance

$$B_a = \frac{-2\lambda}{\eta\pi^2 b}\left(\frac{c}{a}\right)^2 \sum_{m=2}^{\infty}\left[\frac{\sin(m\pi c/a)}{1 - (mc/a)^2}\right]^2 \sqrt{\left(\frac{m}{2}\right)^2 - \left(\frac{a}{\lambda}\right)^2} \tag{4-83}$$

which is plotted in Fig. 4-19. The susceptance is inductive (negative); so the original junction is called an inductive waveguide junction. For single-mode propagation, we must have $a < \lambda$; so our explicit interpretation of the solution is restricted to this range. For wave propagation in the smaller guide, we must have $c > \lambda/2$ if it is air-filled. However, if the smaller guide is dielectric-filled, we can have wave propagation in it when $c < \lambda/2$. Moreover, the aperture susceptance is defined only in terms of E_y in the aperture and has significance independent of the manner in which this E_y is obtained.

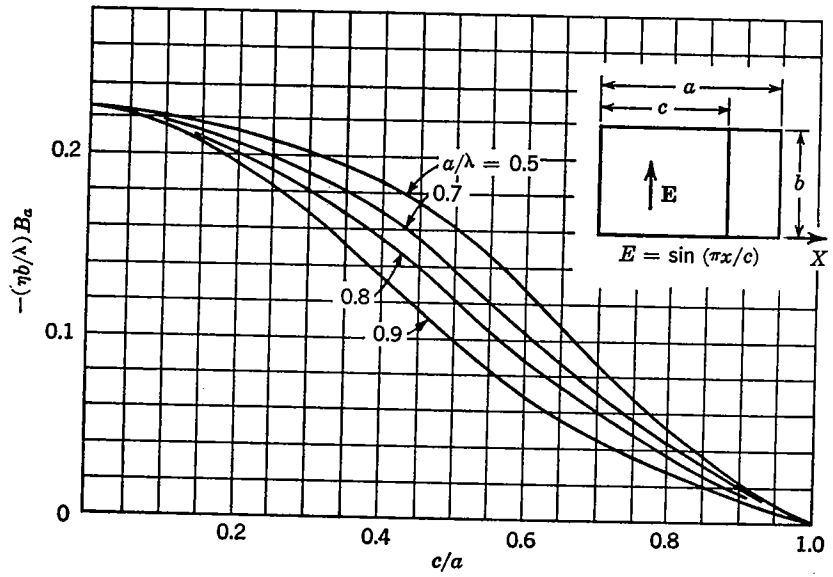

FIG. 4-19. Susceptance of an inductive aperture.

4-10. Currents in Waveguides. The problems of the preceding section might be called "aperture excitation" of waveguides. We shall now consider "current excitation" of waveguides. This involves the determination of modal expansions in terms of current sheets over a guide cross section. The only difference between aperture excitation and current excitation is that the former assumes a knowledge of the tangential electric field and the latter assumes a knowledge of the discontinuity in the tangential magnetic field. The equivalence principle plus duality can be used to transform an aperture-type problem into a current-type problem, and vice versa.

To illustrate the solution, consider a rectangular waveguide with a sheet of x-directed electric currents over the $z = 0$ cross section. This is illustrated by Fig. 3-2, where $\mathbf{J}_s = \mathbf{u}_x f(x,y)$ is now arbitrary. We shall assume that only waves traveling outward from the current are present, that is, the guide is matched in both directions. At $z = 0$ we must have E_x, E_y, and H_x continuous. H_x must also be antisymmetric about $z = 0$; hence it must be identically zero, and it is convenient to use the TMx modes of Sec. 4-4. (Note that $\mathbf{J}$ and its images are x-directed; so it is to be expected that an x-directed $\mathbf{A}$ is sufficient for representing the field.) Superpositions of the TMx modes are

$$\psi^+ = \sum_{m=0}^{\infty}\sum_{n=1}^{\infty} B_{mn}^+ \cos\frac{m\pi x}{a}\sin\frac{n\pi y}{b}\, e^{-\gamma_{mn}z} \qquad z > 0$$

$$\psi^- = \sum_{m=0}^{\infty}\sum_{n=1}^{\infty} B_{mn}^- \cos\frac{m\pi x}{a}\sin\frac{n\pi y}{b}\, e^{\gamma_{mn}z} \qquad z < 0 \tag{4-84}$$

where superscripts + and − refer to the regions $z > 0$ and $z < 0$, respectively. The field in terms of the ψ's is given by Eqs. (4-30). Continuity of E_x and E_y at $z = 0$ requires that

$$B_{mn}^+ = B_{mn}^- = B_{mn} \tag{4-85}$$

The remaining boundary condition is the discontinuity in H_y caused by J_x, which is

$$J_x = [H_y^- - H_y^+]_{z=0} = \sum_{m=0}^{\infty}\sum_{n=1}^{\infty} 2\gamma_{mn}B_{mn}\cos\frac{m\pi x}{a}\sin\frac{n\pi y}{b}$$

This is a Fourier cosine series in x and a Fourier sine series in y. It is evident that $2\gamma_{mn}B_{mn}$ are the Fourier coefficients of J_x, that is,

$$2\gamma_{mn}B_{mn} = J_{mn} = \frac{2\epsilon_m}{ab}\int_0^a dx \int_0^b dy\, J_x \cos\frac{m\pi x}{a}\sin\frac{n\pi y}{b} \qquad (4\text{-}86)$$

This completes the determination of the field. The solution for a y-directed current corresponds to a rotation of axes in the above solution. When both J_x and J_y exist, the solution is a superposition of the two cases $J_y = 0$ and $J_x = 0$. The solution for a magnetic current sheet in the waveguide is obtained in a dual manner. A z-directed electric current can be treated as a loop of magnetic current in the cross-sectional plane, according to Fig. 3-3. A z-directed magnetic current is the dual problem. Thus, we have the formal solution for all possible cases of currents in a rectangular waveguide.

It is also of interest to find the power supplied by the currents in a waveguide. This is most simply obtained from

$$P = -\iint_{z=0} \mathbf{E}\cdot\mathbf{J}_s^*\, ds = -\int_0^a dx\int_0^b dy\, J_x^* E_x\Big|_{z=0}$$

We express J_x in its Fourier series and evaluate E_x by Eqs. (4-30) applied to the above solution. Because of the orthogonality relationships, the power reduces to

$$P = \sum_{m=0}^{\infty}\sum_{n=1}^{\infty} (Z_0)_{mn}|J_{mn}|^2\frac{ab}{4\epsilon_m} \qquad (4\text{-}87)$$

where $(Z_0)_{mn}$ are the TMx wave impedances, given by Eqs. (4-35). This is a summation of the powers that each J_{mn} alone would produce in the guide. In a lossless guide, the power associated with each propagating mode is real, and that associated with a nonpropagating mode is imaginary.

As an example of the above theory, consider the coax to waveguide junction of Fig. 4-20. This is a waveguide "probe feed," the probe being the center conductor of the coax. If the probe is thin, the current on it will have approximately a sinusoidal distribution, as on the linear antenna. With the probe joined to the opposite waveguide wall, as shown in Fig. 4-20, the current maximum is at the joint $x = a$. We therefore assume a current on the probe

$$I(x) \approx \cos k(a - x) \qquad (4\text{-}88)$$

The current sheet approximating this probe is

$$J_x = I(x)\delta(y - c) \qquad (4\text{-}89)$$

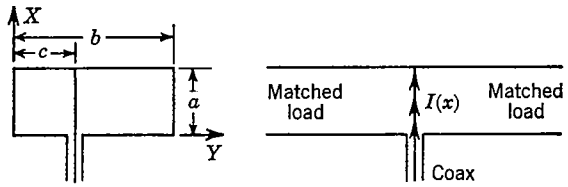

FIG. 4-20. A coax to waveguide junction.

where $\delta(y - c)$ is the impulse function, or delta function (see Appendix C). The Fourier coefficients for the current are then obtained from Eq. (4-86) as

$$J_{mn} = \frac{2\epsilon_m ka\sin ka\sin n\pi c/b}{b[(ka)^2 - (m\pi)^2]} \qquad (4\text{-}90)$$

This, coupled with our earlier formulas, determines the field.

In terms of this solution, let us consider the input impedance seen by the coaxial line. The power supplied by the stub is given by Eq. (4-87). The impedance seen by the coax is then

$$Z_i = \frac{P}{|I_i|^2} = R_i + jX_i$$

where, from Eq. (4-88), the input current is

$$I_i = \cos ka$$

Assume that the waveguide dimensions are such that only the TE_{01} mode propagates. Then only the $m = 0$, $n = 1$ term of Eq. (4-87) is real, and

$$\begin{aligned} R_i &= \frac{ab}{4}\left|\frac{J_{01}}{I_i}\right|^2 (Z_0)_{01} \\ &= \frac{a}{b}(Z_0)_{01}\left(\frac{\tan ka}{ka}\right)^2 \sin^2\frac{\pi c}{b} \end{aligned} \qquad (4\text{-}91)$$

All other terms of the summation of Eq. (4-87) contribute to X_i. However, since we assumed a filamentary current, the series for X_i diverges. To obtain a finite X_i, we must consider a conductor of finite radius. For small a, the reactance will be capacitive. In the vicinity of $a = \lambda/4$, we have a resonance, above which the reactance is inductive. Note that Eq. (4-91) says that the input resistance is infinite at this resonance. This is incorrect for an actual junction, and the error lies in our assumed current. Equation (4-91) gives reliable input resistances only when we are somewhat removed from resonant points. [This is similar to our linear antenna solution (Sec. 2-10)]. Feeds in waveguides with arbitrary terminations are considered in Sec. 8-11.

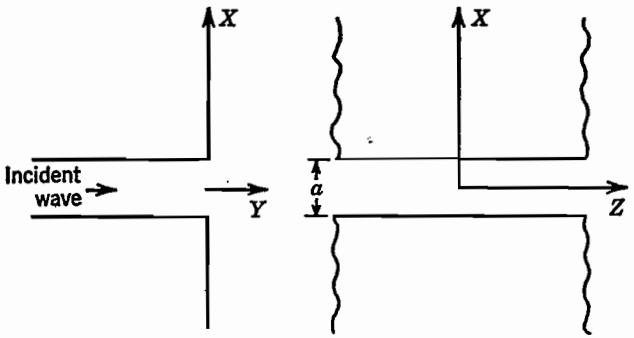

FIG. 4-21. A parallel-plate guide radiating into half-space.

4-11. Apertures in Ground Planes. We have already solved the problem of determining the field from apertures in ground planes, in Sec. 3-6. At this time, however, we shall take an alternative approach and obtain a different form of solution. By the uniqueness theorem, the two forms of solution must be equal. One form may be convenient for some calculations, and the other form for other calculations.

Let us demonstrate the theory for an aperture in the ground plane $y = 0$, illustrated by Fig. 4-21. We further restrict consideration to the case $E_z = 0$, there being only an E_x in the aperture. Taking a clue from our waveguide solution (Sec. 4-9), let us consider Fourier transforms (see Appendix C). The transform pair for E_x over the $y = 0$ plane is

$$\begin{aligned} E_x(x,0,z) &= \frac{1}{4\pi^2}\int_{-\infty}^{\infty} dk_x \int_{-\infty}^{\infty} dk_z\, \bar{E}_x(k_x,k_z)e^{jk_x x}e^{jk_z z} \\ \bar{E}_x(k_x,k_z) &= \int_{-\infty}^{\infty} dx \int_{-\infty}^{\infty} dz\, E_x(x,0,z)e^{-jk_x x}e^{-jk_z z} \end{aligned} \tag{4-92}$$

where a bar over a symbol denotes transform. The form of the transformation suggests that we choose as a wave function

$$\psi = \frac{1}{4\pi^2}\int_{-\infty}^{\infty} dk_x \int_{-\infty}^{\infty} dk_z\, f(k_x,k_z)e^{jk_x x}e^{jk_y y}e^{jk_z z} \tag{4-93}$$

which is a superposition of the form of Eq. (4-9). For our present problem, we take Eq. (4-93) as representing a field TE to z, according to Eqs. (3-89). There is a one-to-one correspondence between a function and its transform; hence it is evident that the transform of ψ is

$$\bar{\psi} = f(k_x,k_z)e^{jk_y y} \tag{4-94}$$

We also can rewrite Eqs. (3-89) in terms of transforms as

$$\begin{aligned} \bar{E}_x &= -jk_y\bar{\psi} & \bar{H}_x &= \frac{-k_x k_z}{j\omega\mu}\bar{\psi} \\ \bar{E}_y &= jk_x\bar{\psi} & \bar{H}_y &= \frac{-k_y k_z}{j\omega\mu}\bar{\psi} \\ \bar{E}_z &= 0 & \bar{H}_z &= \frac{k^2 - k_z^2}{j\omega\mu}\bar{\psi} \end{aligned} \tag{4-95}$$

Specializing the above to the $y = 0$ plane, we have

$$\bar{E}_x|_{y=0} = -jk_y f(k_x,k_z)$$

A comparison of this with Eqs. (4-92) shows that

$$f(k_x,k_z) = \frac{-1}{jk_y}\bar{E}_x(k_x,k_z) \tag{4-96}$$

where $\bar{E}_x$ is given by the second of Eqs. (4-92). This completes the solution. As a word of caution, $k_y = \pm\sqrt{k^2 - k_x^2 - k_z^2}$ is double-valued, and we must choose the correct root. For Eq. (4-94) to remain finite as $y \to \infty$, we must choose

$$k_y = \begin{cases} j\sqrt{k_x^2 + k_z^2 - k^2} & k < \sqrt{k_x^2 + k_z^2} \\ -\sqrt{k^2 - k_x^2 - k_z^2} & k > \sqrt{k_x^2 + k_z^2} \end{cases} \tag{4-97}$$

The minus sign on the lower equality is necessary to remain on the same branch as designated by the upper equality.

The extension of this solution to problems in which both E_x and E_z exist over the $y = 0$ plane can be effected by adding the appropriate TE to x field to the above TE to z field. It can also be obtained as the sum of fields TE and TM to z, or to x, or to y. The case of H_x and H_y specified over the $y = 0$ plane is the dual problem and can be obtained by an interchange of symbols.

For simplicity, we shall choose our illustrative problems to be two-dimensional ones. Let Fig. 4-21 represent a parallel-plate waveguide opening onto a ground plane. If the incident wave is in the transmission-line mode (TEM to y), it is apparent from symmetry that H_z will be the only component of **H**. Let us therefore take H_z as the scalar wave function and construct

$$H_z = \frac{1}{2\pi}\int_{-\infty}^{\infty} f(k_x)e^{jk_x x}e^{jk_y y}\,dk_x \tag{4-98}$$

From this, it is evident that the transform of H_z is

$$\bar{H}_z = f(k_x)e^{jk_y y} \tag{4-99}$$

From the field equations, we relate the transform of **E** to $\bar{H}_z$ as

$$\bar{E}_x = \frac{k_y}{\omega\epsilon}\bar{H}_z \qquad \bar{E}_y = -\frac{k_x}{\omega\epsilon}\bar{H}_z \tag{4-100}$$

Specializing $\bar{E}_x$ to $y = 0$, we have

$$\bar{E}_x\Big|_{y=0} = \frac{k_y}{\omega\epsilon}f(k_x) = \int_{-\infty}^{\infty} E_x(x,0)e^{-jk_x x}\,dx \tag{4-101}$$

from which $f(k_x)$ may be found. For an approximate solution to Fig. 4-21 for $y > 0$, we assume E_x in the aperture to be of the form of the incident mode, that is,

$$E_x\Big|_{y=0} \approx \begin{cases} 1 & |x| < \dfrac{a}{2} \\ 0 & |x| > \dfrac{a}{2} \end{cases} \tag{4-102}$$

Using this in Eq. (4-101), we find

$$\bar{E}_x\Big|_{y=0} = \frac{k_y}{\omega\epsilon}f(k_x) = \frac{2}{k_x}\sin\left(k_x\frac{a}{2}\right) \tag{4-103}$$

To complete the solution, we must also choose the root of k_y for proper behavior as $y \to \infty$. From Eq. (4-99), it is evident that this root is

$$k_y = \begin{cases} j\sqrt{k_x^2 - k^2} & k < |k_x| \\ -\sqrt{k^2 - k_x^2} & k > |k_x| \end{cases} \tag{4-104}$$

The fields are found from the transforms by inversion.

A parameter of interest to us in future work is the aperture admittance. To evaluate this, we shall make use of the integral form of Parseval's theorem (Appendix C), which is

$$\int_{-\infty}^{\infty} f(x)g^*(x)\,dx = \frac{1}{2\pi}\int_{-\infty}^{\infty} \bar{f}(k)\bar{g}^*(k)\,dk$$

We can express the power per unit width (z direction) transmitted by the aperture as

$$P = -\int_{-\infty}^{\infty} [E_x H_z^*]_{y=0}\,dx = -\frac{1}{2\pi}\int_{-\infty}^{\infty} [\bar{E}_x\bar{H}_z^*]_{y=0}\,dk_x$$

From Eqs. (4-100) and (4-102), this becomes

$$P = -\frac{\omega\epsilon}{2\pi}\int_{-\infty}^{\infty}\frac{1}{k_y^*}\,|\bar{E}_x|^2\,dk_x = -\frac{4}{\lambda\eta}\int_{-\infty}^{\infty}\frac{\sin^2(k_x a/2)}{k_y^* k_x^2}\,dk_x$$

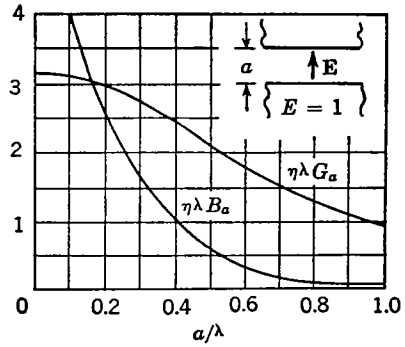

FIG. 4-22. Aperture admittance of a capacitive slot radiator.

We now define the aperture admittance referred to the aperture voltage $V = a$ as

$$Y_a = \frac{P^*}{|V|^2} = \frac{-4}{\lambda\eta a^2}\int_{-\infty}^{\infty}\frac{\sin^2(k_x a/2)}{k_y k_x^2}\,dk_x$$

Note that, by Eq. (4-104), the above integrand is real for $|k_x| < k$ and imaginary for $|k_x| > k$. We can therefore separate Y_a into its real and imaginary parts as

$$G_a = \frac{4}{\lambda\eta a^2}\int_{-k}^{k}\frac{\sin^2(k_x a/2)}{k_x^2\sqrt{k^2 - k_x^2}}\,dk_x$$
$$B_a = \frac{4}{\lambda\eta a^2}\left(\int_{-\infty}^{-k} + \int_{k}^{\infty}\right)\frac{\sin^2(k_x a/2)}{k_x^2\sqrt{k_x^2 - k^2}}\,dk_x$$

The above integrals can be simplified to give

$$\lambda\eta G_a = 2\int_0^{ka/2}\frac{\sin^2 w\,dw}{w^2\sqrt{(ka/2)^2 - w^2}}$$
$$\lambda\eta B_a = 2\int_{ka/2}^{\infty}\frac{\sin^2 w\,dw}{w^2\sqrt{w^2 - (ka/2)^2}} \tag{4-105}$$

For small ka, these are[1]

$$\left.\begin{aligned}\lambda\eta G_a &\approx \pi\left[1 - \frac{(ka)^2}{24}\right] \\ \lambda\eta B_a &\approx 3.135 - 2\log ka\end{aligned}\right\} \quad \frac{a}{\lambda} < 0.1 \tag{4-106}$$

For intermediate ka, the aperture conductance and susceptance are plotted in Fig. 4-22. For large ka, we have

[1] The formula for B_a is a quasi-static result. The direct specialization of the second of Eqs. (4-105) to small ka gives a numerical factor of 4.232 instead of 3.135.

$$\left.\begin{aligned} \lambda\eta G_a &\approx \frac{\lambda}{a} \\ \lambda\eta B_a &\approx \left(\frac{\lambda}{\pi a}\right)^2 \left[1 - \frac{1}{2}\sqrt{\frac{\lambda}{a}} \cos\left(\frac{2a}{\lambda} + \frac{1}{4}\right)\pi\right] \end{aligned}\right\} \quad \frac{a}{\lambda} > 1 \quad (4\text{-}107)$$

The aperture is capacitive, since B_a is always positive.

Another problem of practical interest is that of Fig. 4-21 when the incident wave is in the dominant TE mode (TE to y). In this case, E_z will be the only component of **E**, and we shall take E_z as our scalar wave function. Analogous to the preceding problem, we construct

$$E_z = \frac{1}{2\pi} \int_{-\infty}^{\infty} f(k_x) e^{jk_x x} e^{jk_y y}\, dk_x \quad (4\text{-}108)$$

In terms of Fourier transforms, this is

$$\bar{E}_z = f(k_x) e^{jk_y y} \quad (4\text{-}109)$$

From the field equations, we find the transform of **H** to be

$$\bar{H}_x = \frac{-k_y}{\omega\mu} \bar{E}_z \qquad \bar{H}_y = \frac{k_x}{\omega\mu} \bar{E}_z \quad (4\text{-}110)$$

The $f(k_x)$ is evaluated by specializing Eq. (4-109) to $y = 0$, which gives

$$\bar{E}_z\Big|_{y=0} = f(k_x) = \int_{-\infty}^{\infty} E_z(x,0) e^{-jk_x x}\, dx \quad (4\text{-}111)$$

For an approximate solution, we assume the E_z in the aperture of Fig. 4-21 to be that of the incident TE mode, that is,

$$E_z\Big|_{y=0} \approx \begin{cases} \cos\dfrac{\pi x}{a} & |x| < \dfrac{a}{2} \\ 0 & |x| > \dfrac{a}{2} \end{cases} \quad (4\text{-}112)$$

Substituting this into the preceding equation, we find

$$\bar{E}_z\Big|_{y=0} = f(k_x) = \frac{2\pi a \cos(k_x a/2)}{\pi^2 - (k_x a)^2} \quad (4\text{-}113)$$

The choice of the root for k_y is the same as in the preceding example, given by Eq. (4-104). This completes the formal solution.

Let us again calculate the aperture admittance. The power transmitted by the aperture is

$$P = \int_{-\infty}^{\infty} [E_z H_x^*]_{y=0}\, dx = \frac{1}{2\pi} \int_{-\infty}^{\infty} [\bar{E}_z \bar{H}_x^*]_{y=0}\, dk_x$$

where we have used Parseval's theorem. From Eqs. (4-110) and (4-113),

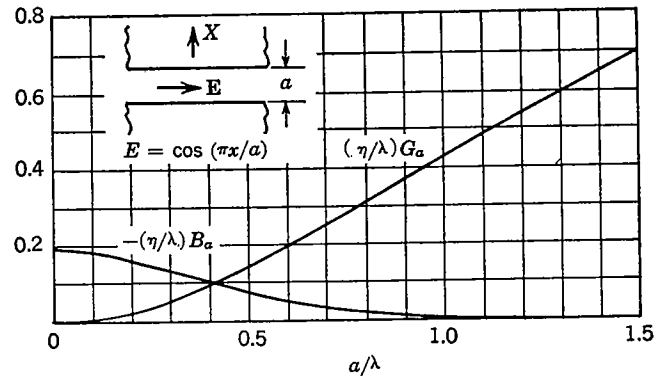

FIG. 4-23. Aperture admittance of an inductive slot radiator.

this becomes

$$P = \frac{-1}{2\pi\omega\mu} \int_{-\infty}^{\infty} k_y^* |\bar{E}_z|^2\, dk_x = \frac{-2\pi a^2}{\omega\mu} \int_{-\infty}^{\infty} \frac{k_y^* \cos^2(k_x a/2)}{[\pi^2 - (k_x a)^2]^2}\, dk_x$$

We shall refer the aperture admittance to the voltage per unit length of the aperture, which is $V = 1$. This gives

$$Y_a = \frac{P^*}{|V|^2} = \frac{-2\pi a^2}{\omega\mu} \int_{-\infty}^{\infty} \frac{k_y \cos^2(k_x a/2)}{[\pi^2 - (k_x a)^2]^2}\, dk_x$$

The integrand is real for $|k_x| < k$ and imaginary for $|k_x| > k$. A separation of Y_a into real and imaginary parts is therefore accomplished in the same manner as in the preceding example. The result is

$$\begin{aligned} \frac{\eta}{\lambda} G_a &= \frac{1}{2} \int_0^{ka/2} \frac{\sqrt{(ka/2)^2 - w^2} \cos^2 w}{[(\pi/2)^2 - w^2]^2}\, dw \\ \frac{\eta}{\lambda} B_a &= \frac{-1}{2} \int_{ka/2}^{\infty} \frac{\sqrt{w^2 - (ka/2)^2} \cos^2 w}{[(\pi/2)^2 - w^2]^2}\, dw \end{aligned} \quad (4\text{-}114)$$

For small ka, we have

$$\left.\begin{aligned} \frac{\eta}{\lambda} G_a &\approx \frac{2}{\pi}\left(\frac{a}{\lambda}\right)^2 \\ \frac{\eta}{\lambda} B_a &\approx -0.194 \end{aligned}\right\} \quad \frac{a}{\lambda} < 0.1 \quad (4\text{-}115)$$

For intermediate ka, the aperture conductance and susceptance are plotted in Fig. 4-23. For large ka,

$$\frac{\eta}{\lambda} G_a \approx \frac{a}{2\lambda} \qquad \frac{a}{\lambda} > 1.5 \quad (4\text{-}116)$$

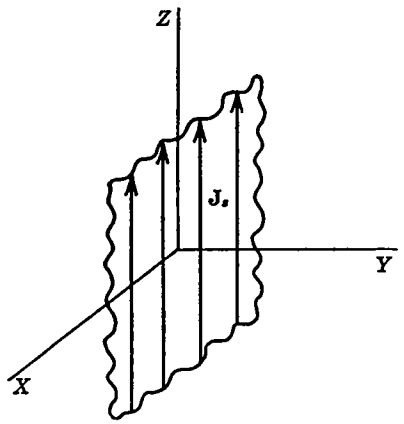

FIG. 4-24. A sheet of z-directed currents in the $y = 0$ plane.

and B_a is negligible. The aperture is inductive since B_a is always negative.

4-12. Plane Current Sheets. The field of plane sheets of current can, of course, be determined by the potential integral method of Sec. 2-9. We now reconsider the problem from the alternative approach of constructing transforms. The procedure is similar to that used in the preceding section for apertures. In fact, if the equivalence principle plus image theory is applied to the results of the preceding section, we have complete duality between apertures (magnetic current sheets) and electric current sheets. However, rather than taking this short cut, let us follow the more circuitous path of constructing the solution from basic concepts.

Suppose we have a sheet of z-directed electric currents over a portion of the $y = 0$ plane, as suggested by Fig. 4-24. The field can be expressed in terms of a wave function representing the z-component of magnetic vector potential. (This we know from the potential integral solution.) The problem is of the radiation type, requiring continuous distributions of eigenvalues. We anticipate the wave functions to be of the transform type, such as Eq. (4-93). From Eqs. (3-86), we have the transforms of the field components for the TM to z field, given by

$$\begin{aligned} \bar{H}_x &= jk_y\bar{\psi} & \bar{E}_x &= \frac{-k_xk_z}{j\omega\epsilon}\bar{\psi} \\ \bar{H}_y &= -jk_x\bar{\psi} & \bar{E}_y &= \frac{-k_yk_z}{j\omega\epsilon}\bar{\psi} \\ \bar{H}_z &= 0 & \bar{E}_z &= \frac{k^2 - k_z^2}{j\omega\epsilon}\bar{\psi} \end{aligned} \tag{4-117}$$

These are dual to Eqs. (4-95). We construct the transform of ψ as

$$\begin{aligned} \psi^+ &= f^+(k_x,k_z)e^{jk_y^+y} & y > 0 \\ \psi^- &= f^-(k_x,k_z)e^{jk_y^-y} & y < 0 \end{aligned} \tag{4-118}$$

For the proper behavior of the fields at large $|y|$, we must choose k_y^+, as in Eq. (4-97), and k_y^- as the other root. That is,

$$k_y^+ = -k_y^- = \begin{cases} j\sqrt{k_x^2 + k_z^2 - k^2} & k < \sqrt{k_x^2 + k_z^2} \\ -\sqrt{k^2 - k_x^2 - k_z^2} & k > \sqrt{k_x^2 + k_z^2} \end{cases} \tag{4-119}$$

Our boundary conditions at the current sheet are continuity of E_x and E_y, and a discontinuity in H_x, according to Eq. (1-86). The boundary condition on E_x and E_y leads to $f^+ = f^-$, and the boundary condition on H_z then leads to

$$f^+(k_x,k_z) = f^-(k_x,k_z) = \frac{j}{2k_y^+}\bar{J}_z \tag{4-120}$$

where $\bar{J}_z$, the transform of J_z, is

$$\bar{J}_z(k_x,k_z) = \int_{-\infty}^{\infty}\int_{-\infty}^{\infty} J_z(x,z)e^{-jk_xx}e^{-jk_zz}\,dx\,dz \tag{4-121}$$

This completes the determination of the field transforms. The field is given by the inverse transformation.

Our two solutions (potential integral and transform) plus the uniqueness theorem can be used to establish mathematical identities. For example, consider the current element of Fig. 2-21. The potential integral solution is $\mathbf{A} = \mathbf{u}_z\psi$ where

$$\begin{aligned} \psi &= \frac{Ile^{-jkr}}{4\pi r} \\ r &= \sqrt{x^2 + y^2 + z^2} \end{aligned} \tag{4-122}$$

For the transform solution,

$$\begin{aligned} J_z &= Il\,\delta(x)\,\delta(z) \\ \bar{J}_z &= \frac{1}{4\pi^2}\int_{-\infty}^{\infty}\int_{-\infty}^{\infty} J_ze^{-jk_xx}e^{-jk_zz}\,dx\,dz = \frac{Il}{4\pi^2} \end{aligned}$$

Hence, for $y > 0$ we have $\mathbf{A} = \mathbf{u}_z\psi$ where

$$\psi = \frac{jIl}{8\pi^2}\int_{-\infty}^{\infty}\int_{-\infty}^{\infty}\frac{1}{k_y}e^{jk_xx}e^{jk_yy}e^{jk_zz}\,dk_x\,dk_z \tag{4-123}$$

where $k_y = k_y^+$ is given by Eq. (4-119). In this example, ψ as well as the

field is unique. Hence, equating Eqs. (4-122) and (4-123), we have the identity

$$\frac{e^{-jkr}}{r} = \frac{1}{2\pi j}\int_{-\infty}^{\infty}\int_{-\infty}^{\infty}\frac{e^{-jy\sqrt{k^2-k_x^2-k_z^2}}}{\sqrt{k^2-k_x^2-k_z^2}}e^{jk_x x}e^{jk_z z}\,dk_x\,dk_z \qquad (4\text{-}124)$$

This holds for all y, since k_y changes sign as y changes sign.

We have considered explicitly only sheets of z-directed current. The solution for x-directed current can be obtained by a rotation of coordinates. When the current sheet has both x and z components, the solution is a superposition of the x-directed case and the z-directed case. The solution for magnetic current sheets is dual to that for electric current sheets. Finally, if the sheet contains y-directed electric currents, we can convert to the equivalent x- and z-directed magnetic current sheet for a solution, and vice versa for y-directed magnetic currents.

A two-dimensional problem to which we shall have occasion to refer in the next chapter is that of a ribbon of axially directed current, uniformly distributed. This is shown in Fig. 4-25. The parameter of interest to us is the "impedance per unit length," defined by

$$Z = \frac{P}{|I|^2} \qquad (4\text{-}125)$$

where P is the complex power per unit length and I is the total current. Rather than work through the details, let us apply duality to the aperture problem of Fig. 4-22. According to the concepts of Sec. 3-6, the field $y > 0$ is unchanged if the aperture is replaced by a magnetic current ribbon $K = 2V$. This ribbon radiates into whole space; so the power per unit length is twice that from the aperture. The admittance of the magnetic current ribbon is thus

$$Y_{\text{mag rib}} = \frac{P^*}{|K|^2} = \frac{2P^*_{\text{apert}}}{|2V|^2} = \tfrac{1}{2}Y_{\text{apert}}$$

where the aperture admittance

$$Y_{\text{apert}} = G_a + jB_a$$

is given by Eq. (4-105), which we can represent by

$$Y_{\text{apert}} = \frac{1}{\eta\lambda}f(ka)$$

By duality, we have the radiation impedance of the electric current ribbon given by

$$Z_{\text{elec rib}} = \frac{1}{2}\frac{\eta}{\lambda}f(ka) = \frac{\eta^2}{2}Y_{\text{apert}} \qquad (4\text{-}126)$$

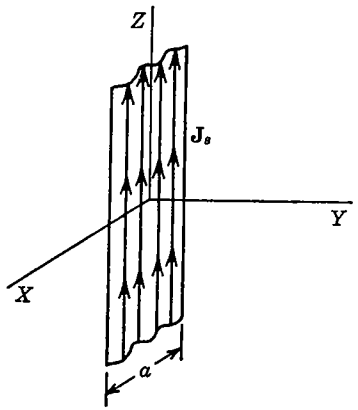

FIG. 4-25. A ribbon of current.

(Compare this with Prob. 3-7. The factor-of-two difference arises because the aperture of Fig. 4-22 radiates into half-space and the twin-slot line sees all-space.) For narrow ribbons, we have from Eqs. (4-106) and (4-126)

$$Z_{\text{elec rib}} \xrightarrow[ka\to 0]{} \frac{\eta}{2\lambda}[\pi + j(3.135 - 2\log ka)] \qquad (4\text{-}127)$$

This we shall compare to the corresponding Z for a cylinder of current in Sec. 5-6.

PROBLEMS

4-1. Show that Eq. (4-9) is a solution to the scalar Helmholtz equation.

4-2. For $k = \beta - j\alpha$, show that

$$\sin kx = \sin \beta x \cosh \alpha x - j\cos \beta x \sinh \alpha x$$
$$\cos kx = \cos \beta x \cosh \alpha x + j\sin \beta x \sinh \alpha x$$

4-3. Derive Eqs. (4-17).

4-4. Following the method used to establish Eq. (2-93), show that the attenuation constant due to conductor losses in a rectangular waveguide is given by Eq. (2-93) for all TE_{0n} modes and by

$$(\alpha_c)_{mn} = \frac{2\mathcal{R}}{\eta}\left[\frac{(a+b)(f_c/f)^2}{ab\sqrt{1-(f_c/f)^2}} + \sqrt{1-\left(\frac{f_c}{f}\right)^2}\,\frac{bm^2+an^2}{b^2m^2+a^2n^2}\right]$$

for TE_{mn} modes, m and n nonzero, and by

$$(\alpha_c)_{mn} = \frac{2\mathcal{R}}{\eta ab\sqrt{1-(f_c/f)^2}}\,\frac{m^2b^3+n^2a^3}{m^2b^2+n^2a^2}$$

for TM_{mn} modes.

4-5. An air-filled rectangular waveguide is needed for operation at 10,000 megacycles. It is desired to have single-mode operation over a 2:1 frequency range, with center frequency 10,000 megacycles. It is also desired to have maximum power-handling capacity under these conditions. Determine the waveguide dimensions and the attenuation constant of the propagating mode for copper walls.

4-6. For a parallel-plate waveguide formed by conductors covering the $y = 0$ and $y = b$ planes, show that

$$\psi_n^{\text{TE}} = \cos\frac{n\pi y}{b}e^{-jk_z z} \qquad n = 1, 2, 3, \ldots$$

are the mode functions generating the two-dimensional TE_n modes according to Eqs. (3-89), and

$$\psi_n^{\text{TM}} = \sin\frac{n\pi y}{b}e^{-jk_z z} \qquad n = 1, 2, 3, \ldots$$

are the mode functions generating the two-dimensional TM_n modes according to Eqs. (3-86). Show that the TEM mode is generated by

$$\psi_0^{\text{TM}} = ye^{-jkz}$$

4-7. Show that an alternative set of mode functions for the parallel-plate waveguide of Prob. 4-6 are

$$\psi_n^{\mathrm{TE}x} = \cos\frac{n\pi y}{b}\, e^{-ik_z z} \qquad n = 0, 1, 2, \ldots$$

which generate the TEx_n modes according to Eqs. (4-32), and

$$\psi_n^{\mathrm{TM}x} = \sin\frac{n\pi y}{b}\, e^{-ik_z z} \qquad n = 1, 2, 3, \ldots$$

which generate the TMx_n modes according to Eqs. (4-30). Note that $n = 0$ in the above TEx mode function gives the TEM mode.

4-8. Show that the TEx and TMx modes of Sec. 4-4 are linear combinations of the TE and TM modes of Sec. 4-3, that is,

$$\mathbf{E}_{mn}^{\mathrm{TE}x} = A(\mathbf{E}_{mn}^{\mathrm{TE}} + B\mathbf{E}_{mn}^{\mathrm{TM}})$$
$$\mathbf{H}_{mn}^{\mathrm{TM}x} = C(\mathbf{H}_{mn}^{\mathrm{TE}} + D\mathbf{H}_{mn}^{\mathrm{TM}})$$

Determine A, B, C, and D.

4-9. Show that the resonant frequencies of the two-dimensional (no z variation) resonator formed by conducting plates over the $x = 0$, $x = a$, $y = 0$, and $y = b$ planes are the cutoff frequencies of the rectangular waveguide.

4-10. Following the method used to establish Eq. (2-101), show that the Q due to conductor losses for the various modes in a rectangular cavity are

$$(Q_c)_{0np}^{\mathrm{TE}} = \frac{\eta abck_r^3}{2\mathcal{R}(bck_r^2 + 2ack_y^2 + 2abk_z^2)}$$

$$(Q_c)_{m0p}^{\mathrm{TE}} = \frac{\eta abck_r^3}{2\mathcal{R}(ack_r^2 + 2bck_x^2 + 2abk_z^2)}$$

$$(Q_c)_{mnp}^{\mathrm{TE}} = \frac{\eta abck_{xy}^2k_r^3}{4\mathcal{R}[bc(k_{xy}^4 + k_y^2k_z^2) + ac(k_{xy}^4 + k_x^2k_z^2) + abk_{xy}^2k_z^2]}$$

$$(Q_c)_{mn0}^{\mathrm{TM}} = \frac{\eta abck_r^3}{2\mathcal{R}(abk_r^2 + 2bck_x^2 + 2ack_y^2)}$$

$$(Q_c)_{mnp}^{\mathrm{TM}} = \frac{\eta abck_{xy}^2k_r}{4\mathcal{R}[b(a + c)k_x^2 + a(b + c)k_y^2]}$$

where

$$k_x = \frac{m\pi}{a} \qquad k_y = \frac{n\pi}{b} \qquad k_z = \frac{p\pi}{c}$$
$$k_{xy} = \sqrt{k_x^2 + k_y^2} \qquad k_r = \sqrt{k_x^2 + k_y^2 + k_z^2}$$

4-11. Calculate the first ten higher-order resonant frequencies for the rectangular cavity of Prob. 2-38.

4-12. Consider the two-dimensional parallel-plate waveguide formed by conductors over the $x = 0$ and $x = a$ planes, and dielectrics ϵ_1 for $0 < x < d$ and ϵ_2 for $d < x < a$. Show that for modes TM to x the characteristic equation is Eq. (4-45) with

$$k_{x1} = \sqrt{\omega^2\epsilon_1\mu_1 - k_z^2} \qquad k_{x2} = \sqrt{\omega^2\epsilon_2\mu_2 - k_z^2}$$

and for modes TE to x the characteristic equation is Eq. (4-47). Note that no mode TEM to z (the direction of propagation) is possible.

4-13. Show that the lowest-order TM to x mode of Prob. 4-12 reduces to the transmission-line mode either as $\epsilon_1 \to \epsilon_2$ and $\mu_1 \to \mu_2$ or as $d \to 0$. Show that, if $a \ll \lambda_2$,

$$k_z \approx \omega\sqrt{\frac{\epsilon_1\epsilon_2[\mu_1 d + \mu_2(a - d)]}{\epsilon_1(a - d) + \epsilon_2 d}}$$

for the dominant mode. Show that the static inductance and capacitance per unit width and length of the transmission line are

$$L = \mu_1 d + \mu_2(a - d) \qquad C = \frac{\epsilon_1\epsilon_2}{\epsilon_1(a - d) + \epsilon_2 d}$$

The usual transmission-line formula $k_z = \omega\sqrt{LC}$ therefore applies if a is small. Also, the field is almost TEM.

4-14. Consider the dominant mode of the partially filled guide (Fig. 4-6) for $b > a$. When d is small, Eq. (4-45) can be approximated by Eq. (4-48) for the dominant mode. Denote the empty-guide propagation constant ($d = 0$) by

$$\beta_0 = \sqrt{k_2^2 - \left(\frac{\pi}{b}\right)^2}$$

and show, from the Taylor expansion of Eq. (4-48) about $d = 0$ and $k_z = \beta_0$, that for small d

$$k_z = \beta_0 + \frac{\epsilon_2}{\epsilon_1}\left(\frac{k_1^2 - k_2^2}{2\beta_0}\right)\frac{d}{a}$$

4-15. Consider the dominant mode of the partially filled guide (Fig. 4-6) for $a > b$. Denote the empty-guide propagation constant ($d = 0$) by

$$\beta_0 = \sqrt{k_2^2 - \left(\frac{\pi}{a}\right)^2}$$

and show, from the Taylor expansion of the reciprocal of Eq. (4-47) about $d = 0$ and $k_z = \beta_0$, that for small d

$$k_z = \beta_0 + \frac{\mu_1 - \mu_2}{\mu_2\beta_0}\left(\frac{\pi}{a}\right)^2\frac{d}{a} + \frac{\pi^2\mu_1}{3\mu_2\beta_0}(k_1^2 - k_2^2)\left(\frac{d}{a}\right)^3$$

4-16. Show that the resonant frequencies of a partially filled rectangular cavity (Fig. 4-6 with additional conductors covering the $z = 0$ and $z = c$ planes) are solutions to Eqs. (4-45) and (4-47) with

$$k_{x1}^2 + \left(\frac{n\pi}{b}\right)^2 + \left(\frac{p\pi}{c}\right)^2 = k_1^2$$
$$k_{x2}^2 + \left(\frac{n\pi}{b}\right)^2 + \left(\frac{p\pi}{c}\right)^2 = k_2^2$$

where $n = 0, 1, 2, \ldots$; $p = 0, 1, 2, \ldots$; $n = p = 0$ excepted.

4-17. For the partially filled cavity of Prob. 4-16, show that if $c > b > a$, the resonant frequency of the dominant mode for small d is given by

$$\omega_r = \omega_0\left[1 - \frac{1}{2}\left(\frac{\mu_1}{\mu_2} - \frac{\epsilon_2}{\epsilon_1}\right)\frac{d}{a}\right]$$

where ω_0 is the resonant frequency of the empty cavity,

$$\omega_0 = \frac{1}{\sqrt{\epsilon_2\mu_2}} \sqrt{\left(\frac{\pi}{b}\right)^2 + \left(\frac{\pi}{c}\right)^2}$$

Hint: Use the results of Prob. 4-14.

4-18. For the partially filled cavity of Prob. 4-16, show that if $c > a > b$, the resonant frequency of the dominant mode for small d is given by

$$\omega = \omega_0 \left[1 - \frac{\mu_1 - \mu_2}{\mu_2} \frac{c^2}{a^2 + c^2} \frac{d}{a} - \frac{\pi^2\mu_1}{3\mu_2} \left(\frac{\epsilon_1\mu_1}{\epsilon_2\mu_2} - 1\right) \left(\frac{d}{a}\right)^3\right]$$

where ω_0 is the resonant frequency of the empty cavity

$$\omega_0 = \frac{1}{\sqrt{\epsilon_2\mu_2}} \sqrt{\left(\frac{\pi}{a}\right)^2 + \left(\frac{\pi}{c}\right)^2}$$

Hint: Use the results of Prob. 4-15.

4-19. Consider a rectangular waveguide with a centered dielectric slab, as shown in the insert of Fig. 7-10. Show that the characteristic equation for determining the propagation constants of modes TE to x is

$$\frac{k_{x0}}{\mu_0} \cot\left(k_{x0} \frac{a - d}{2}\right) = \frac{k_{x1}}{\mu_1} \tan\left(k_{x1} \frac{d}{2}\right)$$

and for modes TM to x it is

$$\frac{k_{x0}}{\epsilon_0} \tan\left(k_{x0} \frac{a - d}{2}\right) = \frac{k_{x1}}{\epsilon_1} \cot\left(k_{x1} \frac{d}{2}\right)$$

where

$$k_{x0}^2 + \left(\frac{n\pi}{b}\right)^2 + k_z^2 = k_0^2 = \omega^2\epsilon_0\mu_0$$

$$k_{x1}^2 + \left(\frac{n\pi}{b}\right)^2 + k_z^2 = k_1^2 = \omega^2\epsilon_1\mu_1$$

The dominant mode is the lowest-order TE mode (smallest root for $n = 0$).

4-20. Derive Eq. (4-58).

4-21. A plane slab of polystyrene ($\epsilon_r = 2.56$) is ¾ centimeter thick. What slab-guide modes will propagate unattenuated at a frequency of 30,000 megacycles? Calculate the cutoff frequencies of these modes. Using Fig. 4-11, determine the propagation constants of the propagating TE modes at 30,000 megacycles. Determine the propagation constants of the propagating TM modes by numerical solution of Eq. (4-56) or (4-58). How can the cutoff frequencies of corresponding TE and TM modes be the same, yet the propagation constants be different?

4-22. By a Taylor expansion of Eq. (4-56) about $a = 0$, $v = 0$, show that the dominant TM mode of the slab guide (Fig. 4-10) is characterized by

$$v = \frac{\epsilon_0}{\epsilon_d} (k_d^2 - k_0^2) \frac{a}{2}$$

for small a. Similarly, show that the dominant TE mode is characterized by

$$v = \frac{\mu_0}{\mu_d} (k_d^2 - k_0^2) \frac{a}{2}$$

for small a. In each case, the propagation constant is given by

$$k_z = k_0 + \frac{v^2}{2k_0}$$

4-23. A plane conductor has been coated with shellac ($\epsilon_r = 3.0$) to a thickness of 0.005 inch. It is to be used in a 30,000-megacycle field. Will any tightly bound surface wave be possible? Calculate the attenuation constant in the direction perpendicular to the coated conductor.

4-24. For the corrugated conductor of Fig. 4-15, it is desired that the field be attenuated to 36.8 per cent of its surface value at one wavelength from the surface. Determine the minimum depth of slot needed.

4-25. Suppose that the slots of the corrugated conductor of Fig. 4-15 are filled with a dielectric characterized by ϵ_d, μ_d. Show that for this case

$$v = \frac{\epsilon_0}{\epsilon_d} k_d \tan k_d d$$

$$k_z = k_0 \sqrt{1 + \frac{\epsilon_0\mu_d}{\epsilon_d\mu_0} \tan^2 k_d d}$$

where $k_d = \omega\sqrt{\epsilon_d\mu_d}$.

4-26. Use the TEx mode functions of Prob. 4-7 for the parallel-plate waveguide formed by conductors covering the $y = 0$ and $y = b$ planes. Show that a field having no E_z is given by Eqs. (4-32) with

$$\psi = \sum_{n=0}^{\infty} A_n \cos\frac{n\pi y}{b} e^{-\gamma_n z} \qquad z > 0$$

where

$$A_n = \frac{\epsilon_n}{b\gamma_n} \int_0^b E_y\Big|_{z=0} \cos\frac{n\pi y}{b}\, dy$$

4-27. Consider the junction of two parallel-plate transmission lines of height c for $z < 0$ and height b for $z > 0$, with the bottom plate continuous. (The cross section is that of the second drawing of Fig. 4-16.) Using the formulation of Prob. 4-26, show that the aperture susceptance per unit width referred to the aperture voltage is

$$B_a \approx \frac{4}{\eta\lambda} \sum_{n=1}^{\infty} \frac{\sin^2(n\pi c/b)}{(n\pi c/b)^2 \sqrt{n^2 - (2b/\lambda)^2}}$$

where a constant E_y has been assumed in the aperture. Compare this with Eq. (4-78).

4-28. The centered capacitive waveguide junction is shown in Fig. 4-26. Show that the aperture susceptance referred to the maximum aperture voltage is given by Eq. (4-78) with λ_g replaced by $2\lambda_g$. It is assumed that E_y in the aperture is that of the incident mode.

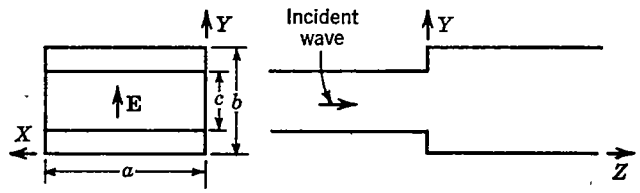

FIG. 4-26. A centered capacitive waveguide junction

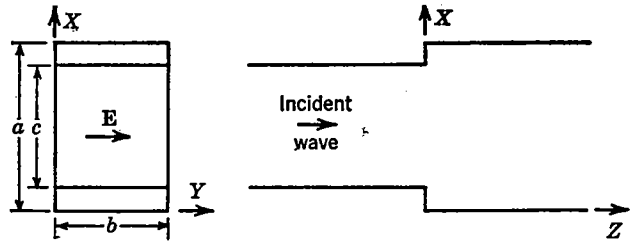

FIG. 4-27. A centered inductive waveguide junction.

4-29. Consider the centered inductive waveguide junction of Fig. 4-27. Assuming that E_y in the aperture is that of the incident mode, show that the aperture susceptance referred to the maximum aperture voltage is given by

$$B_a \approx \frac{-8\lambda}{\eta\pi^2 b}\left(\frac{c}{a}\right)^2 \sum_{3,5,7,\ldots}^{\infty} \left[\frac{\cos\,(m\pi c/2a)}{1-(mc/a)^2}\right]^2 \sqrt{\left(\frac{m}{2}\right)^2-\left(\frac{a}{\lambda}\right)^2}$$

4-30. In Eq. (4-83), note that as $c/a \to 0$ the summation becomes similar to an integration. Use the analogy $mc/a \sim x$ and $c/a \sim dx$ to show that

$$-\frac{b\eta}{\lambda} B_a \xrightarrow[c/a\to 0]{} \frac{1}{\pi^2}\int_0^\infty \left(\frac{\sin \pi x}{1-x^2}\right)^2 x\,dx$$

Integrate by parts, and use the identity[1]

$$\int_0^\infty \frac{\sin 2\pi x}{x^2-1}\,dx = \int_0^{2\pi}\frac{\sin y}{y}\,dy = \mathrm{Si}(2\pi)$$

to show that

$$-\frac{b\eta}{\lambda} B_a \xrightarrow[c/a\to 0]{} \frac{\mathrm{Si}(2\pi)}{2\pi} = 0.226$$

4-31. Let there be a sheet of y-directed current J_y over the $z = 0$ plane of a parallel-plate waveguide formed by conductors over the $y = 0$ and $y = b$ planes. The guide is matched in both the $+z$ and $-z$ directions. Show that the field produced by the current sheet is

$$\sum_{n=0}^{\infty} A_n \cos\frac{n\pi y}{b}\, e^{-\gamma_n|z|} = \begin{cases} H_x & z > 0 \\ -H_x & z < 0 \end{cases}$$

where

$$A_n = \frac{\epsilon_n}{2b}\int_0^b J_y(y)\cos\frac{n\pi y}{b}\,dy$$

4-32. Let the current sheet of Prob. 4-31 be x-directed instead of y-directed. Show that field produced by this x-directed current sheet is

$$E_x = \sum_{n=1}^{\infty} B_n \sin\frac{n\pi y}{b}\, e^{-\gamma_n|z|}$$

where

$$B_n = \frac{j\omega\mu}{\gamma_n b}\int_0^b J_x(y)\sin\frac{n\pi y}{b}\,dy$$

[1] D. Bierens de Haan, "Nouvelles tables d'intégrales définies," p. 225, table 161, no. 3, Hafner Publishing Company, New York, 1939 (reprint).

4-33. Consider the coax to waveguide junction of Fig. 4-28*a*. Only the TE_{01} mode propagates in the waveguide, which is matched in both directions. Assume that the current on the wire varies as cos (kl), where l is the distance from the end of the wire. Show that the input resistance seen by the coax is

$$R_i = \frac{a}{b}(Z_0)_{01}\left[\frac{\sin\,(\pi c/b)\,\sin kd}{ka\cos k(c+d)}\right]^2$$

where $(Z_0)_{01}$ is the TE_{01} characteristic wave impedance.

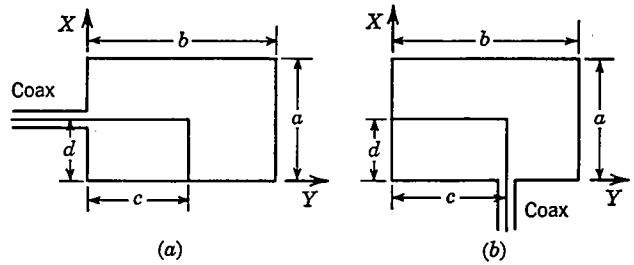

FIG. 4-28. Coax to waveguide junctions.

4-34. Suppose that the coax to waveguide junction of Prob. 4-33 is changed to that of Fig. 4-28*b*. Show that the input resistance seen by the coax is now

$$R_i = \frac{a}{b}(Z_0)_{01}\left\{\frac{\sin\,(\pi c/b)[\sin k(c+d) - \sin kc]}{ka\cos k(c+d)}\right\}^2$$

4-35. By expanding $(\sin w/w)^2$ in a Taylor series about $w = 0$, show that the first of Eqs. (4-105) becomes

$$\lambda\eta G_a = \pi\left[1 - \frac{1}{6}\left(\frac{ka}{2}\right)^2 + \frac{1}{60}\left(\frac{ka}{2}\right)^4 - \frac{1}{1008}\left(\frac{ka}{2}\right)^6 + \cdots\right]$$

4-36. Consider the second of Eqs. (4-105) as the contour integral

$$\lambda\eta B_a = \mathrm{Re}\left[\int_{C_1}\frac{(1-e^{j2w})dw}{w^2\sqrt{w^2-(ka/2)^2}}\right]$$

where C_1 is shown in Fig. 4-29. Consider the closed contour $C_1 + C_2 + C_\infty + C_0$, and express $\lambda\eta B_a$ in terms of a contour integral over C_2 and C_0. Show that as $ka/2$ becomes large, this last contour integral reduces to the second of Eqs. (4-107).

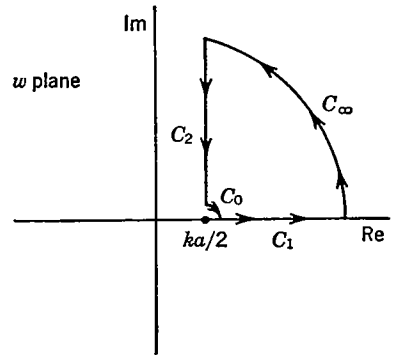

FIG. 4-29. Contours for Prob. 4-36.

4-37. By expanding $\cos^2 w/[(\pi/2)^2 - w^2]^2$ in a Taylor series about $w = 0$, show that the first of Eqs. (4-114) becomes

$$\frac{\eta}{\lambda} G_a = \frac{2}{\pi} \sum_{n=1}^{\infty} b_n \left(\frac{a}{\lambda}\right)^{2n}$$

where

$$\begin{aligned} b_1 &= +1.0 \\ b_2 &= -0.467401 \\ b_3 &= +0.189108 \\ b_4 &= -0.055613 \\ b_5 &= +0.012182 \\ b_6 &= -0.002083 \end{aligned}$$

4-38. Specialize the second of Eqs. (4-114) to the case $a = 0$, integrate by parts, and use the identity (see Prob. 4-30)

$$\int_0^\infty \frac{\sin 2x\, dx}{(\pi/2)^2 - x^2} = \frac{2}{\pi} \int_0^\pi \frac{\sin y}{y}\, dy = \frac{2}{\pi} \operatorname{Si}(\pi)$$

to show that

$$-\frac{\eta}{\lambda} B_a \xrightarrow[a \to 0]{} \frac{1}{2\pi} \operatorname{Si}(\pi) - \frac{2}{\pi^2} = 0.194$$

4-39. Show that the first of Eqs. (4-114) reduces to the contour integral

$$\frac{\eta}{\lambda} G_a \xrightarrow[ka \to \infty]{} \frac{ka}{8} \operatorname{Re}\left[\int_{C_1} \frac{(1 + e^{j2w})\, dw}{[(\pi/2)^2 - w^2]^2}\right]$$

where C_1 is shown in Fig. 4-30. Consider the closed contour $C_1 + C_2 + C_\infty + C_0$, and express G_a in terms of a contour integral over C_2 and C_0. Evaluate this last contour integral, and show that

$$\frac{\eta}{\lambda} G_a \xrightarrow[ka \to \infty]{} \frac{ka}{4\pi}$$

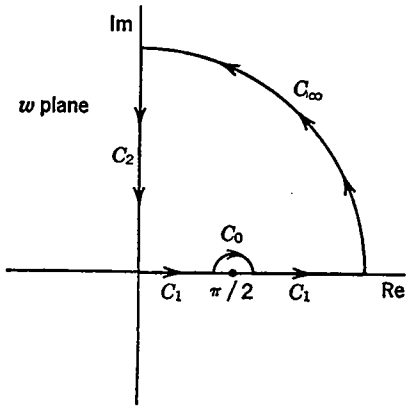

FIG. 4-30. Contours for Prob. 4-39.

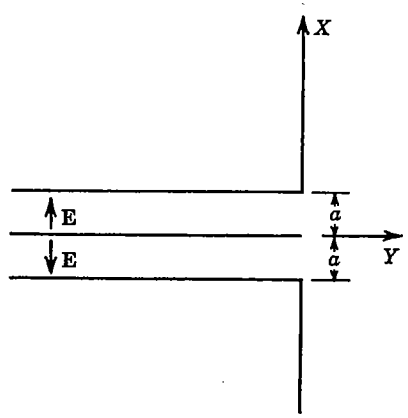

FIG. 4-31. Two parallel-plate transmission lines radiating into half-space.

4-40. Two parallel-plate transmission lines opening onto a conducting plane are excited in opposite phase and equal magnitude, as shown in Fig. 4-31. Assume E_x in the aperture is a constant for each line, and show that the aperture susceptance referred to the aperture voltage of one line is

$$G_a = \frac{8}{\lambda\eta} \int_0^{ka} \frac{\sin^4 w\, dw}{w^2 \sqrt{(ka)^2 - w^2}}$$

$$B_a = \frac{8}{\lambda\eta} \int_{ka}^{\infty} \frac{\sin^4 w\, dw}{w^2 \sqrt{w^2 - (ka)^2}}$$

4-41. Construct the vector potential $\mathbf{A} = \mathbf{u}_z \psi$ for a sheet of z-directed currents over the $y = 0$ plane (Fig. 4-24) by (a) the potential integral method and (b) the transform method. Show by use of Green's second identity [Eq. (3-44)] that the two ψ's are equal. Specialize the potential integral solution to $r \to \infty$, and show that

$$\psi \xrightarrow[r \to \infty]{} \frac{e^{-jkr}}{4\pi r} \tilde{J}_z(-k \cos\phi \sin\theta,\ -k \cos\theta)$$

where $\tilde{J}_z(k_x,k_z)$ is given by Eq. (4-121).

4-42. Suppose that the current in Fig. 4-25 is x-directed rather than z-directed, and of magnitude

$$J_x = \cos\frac{\pi x}{a} \qquad |x| < \frac{a}{2}$$

Show that the impedance per unit length, defined by Eq. (4-125), where I is the current per unit length, is given by Eq. (4-126), where Y_{apert} is now the aperture admittance of Fig. 4-23.